Studies on Geographic DTN Routing with Random Mobile Agents

Daiki Matsui

March 2019

Department of Informatics
Graduate School of Science and Technology
Kwansei Gakuin University

Abstract

In this thesis, we investigate geographic DTN routing with random mobile agents. The main contributions of this thesis are fourfold. First, we derive the average and the distribution of message delivery delay with geographic DTN routing under random walk mobility in small-scale networks. Our analysis reveals the effect of system parameters — the number of mobile agents on the field, the number of message loadings at a geographic location, the message generation rate and the number of message replicas — on the average and the distribution of message delivery delays. Second, we approximately derive the average message delivery delay with geographic DTN routing under random walk mobility in large-scale networks. We show that geographic DTN routing is scalable; i.e., its average message delivery delay is approximately proportional to the network size (i.e., geographic locations) unless heavily loaded. We also show that the network topology has limited impact on the performance of geographic DTN routing except heavily loaded conditions; the average message delivery delay is mostly determined by the degree of the destination node. Third, we derive the mean recurrence time of the CRWP (Constrained Random WayPoint) mobility model to reveal the impact of mobility models on the performance of geographic DTN routing. Fourth, we derive the hitting time of the CRWP mobility model to reveal the characteristics of the CRWP mobility model.

Contents

List of Figures

1 Introduction

Delay/disruption-tolerant networking (DTN), which allows end-to-end node communication even when communication links between nodes are not functioning normally, has recently been regarded as a promising communication technology for realizing communication infrastructure at the time of disaster and low-cost communication infrastructure [1]. DTN aims to achieve end-to-end data transfers in communication environments where inter-node communication links can be temporarily severed, or the transmission delay between nodes can temporarily increase.

In the literature, extensive researches on DTN routing based on store-carry-and-forward communication with mobile nodes have been actively performed [1]. DTN routing communication between mobile nodes generally utilizes the characteristics of mobile nodes, which autonomously and independently move on the field, and also adhoc wireless communication among mobile nodes for realizing end-to-end message delivery.

To the best of our knowledge, most of existing DTN routing algorithms are designed for message delivery between mobile nodes (i.e., message transmission from a mobile node to one or more other mobile nodes) [2, 3]. However, in practical applications of DTNs in several fields, endpoints of communication might not be always *mobile* nodes. In other words, endpoints might also be *fixed* nodes, so other types of communications between mobile and fixed nodes and also between fixed nodes should be required. In this thesis, a class of DTN routing utilizing mobile nodes for store-carry-and-forward communication among fixed nodes is called *geographic DTN routing*.

A geographic DTN routing aims at realization of message delivery among multiple (generally, geographically-dispersed) *geographic locations* on a field

without necessity of specific communication infrastructure by utilizing mobility of *mobile agents*. On the field, there exist multiple geographic locations (i.e., fixed nodes) and mobile agents (i.e., mobile nodes), and messages are transferred among geographic locations using store-carry-and-forward operations of mobile agents.

In the literature, fundamental characteristics of geographic DTN routing with five routing algorithms (Random, Nearest, Farthest, Distant and AOD (Angle Of Deviation)) have been studied through simulation experiments [4].

In this thesis, we investigate geographic DTN routing with random mobile agents. The main contributions of this thesis are fourfold.

First, we derive the average and the distribution of message delivery delay with geographic DTN routing under random walk mobility in small-scale networks. Our analysis reveals the effect of system parameters — the number of mobile agents on the field, the number of message loadings at a geographic location, the message generation rate and the number of message replicas — on the average and the distribution of message delivery delays.

Second, we approximately derive the average message delivery delay with geographic DTN routing under random walk mobility in large-scale networks. We show that geographic DTN routing is scalable; i.e., its average message delivery delay is approximately proportional to the network size (i.e., geographic locations) unless heavily loaded. We also show that the network topology has limited impact on the performance of geographic DTN routing except heavily loaded conditions; the average message delivery delay is mostly determined by the degree of the destination node.

Third, we derive the mean recurrence time of the CRWP (Constrained

Random WayPoint) mobility model to reveal the impact of mobility models on the performance of geographic DTN routing.

Fourth, we derive the hitting time of the CRWP mobility model (i.e., the expected value of the time for an agent on $G = (V, E)$ following the CRWP mobility model from starting his movement on vertex $s \in V$ to reach vertex $t \in V$ at first). We show that the CRWP mobility model can be regarded as a kind of random walk.

The organization of this thesis is as follows. Chapter 2 derives the average and the distribution of message delivery delays in a geographic DTN routing with multiple mobile agents, whose mobility patterns are given by random walks on a graph and message routing algorithm is FIFO (First-In First-Out) algorithm. Chapter 3 approximately derives the average message delivery delay in geographic DTN routing under random walk mobility on a large-scale network. Chapter 4 derives the mean recurrence time of the CRWP mobility model to reveal the impact of mobility models on the performance of geographic DTN routing. Chapter 5 derives hitting time of the CRWP mobility model to reveal the characteristics of the CRWP mobility model. Chapter 6 concludes this thesis and discusses future works.

2 Analysis of Geographic DTN Routing under Random Walk Mobility Model

In this chapter, we derive the average and the distribution of message delivery delays of geographic DTN routing with FIFO algorithm under two workload models by modeling the behaviors of mobile agents as multiple random walks on a graph. In this chapter, two types of workload models — one-time generation (i.e., simultaneous generation at the initial state)

and continuous generation (i.e., Poisson message arrival) — are considered. Our analysis reveals the effect of system parameters — the number of mobile agents on the field, the number of message loadings at a geographic location, the message generation rate and the number of message replicas — on the average and the distribution of message delivery delays.

2.1 Geographic DTN Routing and FIFO Algorithm

In this section, we briefly explain the concept of geographic DTN routing. Refer to [4] for more detailed description.

A geographic DTN routing aims at realization of message delivery among multiple (generally, geographically-dispersed) *geographic locations* on a field without necessity of specific communication infrastructure by utilizing mobility of *mobile agents*. There exist multiple geographic locations and also multiple mobile agents (i.e., mobile nodes) on the field, and messages are carried by mobile agents for message delivery among geographic locations (Fig. 1).

Every geographic location generates messages destined for other geographic locations. We assume that multiple mobile agents autonomously and irregularly visit geographic locations one and another. A mobile agent can *load* a message at its visiting geographic location, carry multiple messages while it moves, and *unload* one or more carrying messages at its visiting geographic location.

There exist a huge number of possible geographic DTN routing algorithms depending on the combination of various factors: message generation patterns and buffer sizes of geographic locations, mobility, mobility controllability, buffer sizes of mobile agents, type and capacity of wireless communications between a geographic location and a mobile agent, and

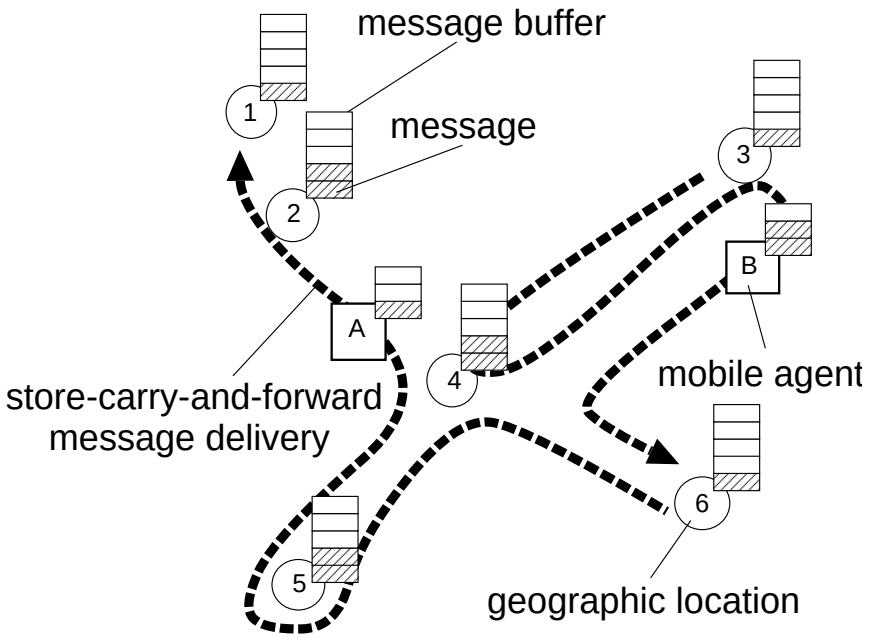

Figure 1: An overview of geographic DTN routing with mobile agents

availability of positional information of mobile agents (e.g., GPS (Global Positioning System)).

In this chapter, we focus on a case where people carrying portable devices such as smartphones autonomously move among geographic locations. Therefore, we assume that mobile agents' mobility are uncontrollable (i.e., a geographic DTN routing algorithm has no control over people's mobility), and the capacity of wireless communication is limited (i.e., the bandwidth for message transfer between a geographic location and a portable device is finite). On the contrary, we assume that the buffer sizes of geographic locations and mobile agents (e.g., portable devices) are sufficiently large. We also assume that the positional information of mobile agents are available to a geographic DTN routing algorithm.

Geographic DTN routing algorithms can be roughly classified by their message loading mechanism (i.e., how messages are copied/moved from

a geographic location) and message unloading mechanism (i.e., how messages are copied/moved from a mobile agent).

In this chapter, we focus on one of the simplest algorithms, FIFO (First-In First Out) algorithm, which should be the baseline for other complex geographic DTN routing algorithms.

FIFO algorithm is the minimal and the simplest algorithm, which performs sequential message loading and no message unloading. When mobile agent m visits geographic location v, at most K oldest messages are chosen from the buffer of geographic location v. Those messages are moved to the buffer of mobile agent m. If mobile agent m has one or more messages destined for geographic location v in its buffer, those messages are moved to the buffer of geographic location v.

2.2 Analytic Model

We model the field comprising of multiple geographic locations and paths connecting those geographic locations as an undirected graph $G = (V, E)$ where vertices and edges correspond to geographic locations and paths, respectively. Let A be the adjacency matrix of G, $d(v)$ be the degree of vertex $v \in V$.

We model the behavior of a mobile agent in geographic DTN routing as a discrete random walk on graph G. At every slot, a mobile agent randomly and synchronously moves one of its neighbor vertices in G. Namely, a mobile agent on vertex v at slot k randomly moves to one of neighbor vertices, vertex v, with probability $1/d(v)$ at slot $k + 1$.

Every mobile agent performs message delivery using FIFO algorithm. When a mobile agent visits a geographic location, it performs the following operations: (1) moves at most K oldest messages from geographic lo-

cation's buffer to mobile agent's buffer (message loading), and (2) moves, if any, all messages destined for the current geographic location from mobile agent's buffer to geographic location's buffer. The freshness of a message is simply determined by the age of the message (i.e., the time elapsed since the time of its generation). In message loading, if there exist multiple messages of the same freshness, any of those messages are randomly selected. In our analysis, it is assumed that the buffer of mobile agents are sufficiently large.

In this chapter, we focus on geographic DTN routing with the number M of mobile agents. The starting vertex of mobile agent m at the initial state ($k = 0$) is denoted by s_m.

There exist two classes of geographic DTN routing: *single-copy* and *multiple-copy*. In the single-copy case, every message is not duplicated in the network. So, a single-copy geographic DTN routing consumes least network resources. However, message delivery delays in the single-copy case tend to be large, and the message delivery probability from the originating node to the destination node is generally low. For accelerating message delivery and increasing the likelihood of message delivery, a message is duplicated in the multiple-copy case. In this chapter, the number of replicas for a message is denoted by C.

We consider two workload models: *one-time* and *continuous* workload models.

- One-time workload model

  In one-time workload model, a fixed number of messages are simultaneously generated at the initial state. At the initial state, all messages are initially placed in buffers of their originating geographic locations. Namely, no additional message is generated at $k \geq 1$. Let

$N_{u,v}$ be the number of messages generated at u and destined for v. Let N_u ($\equiv \sum_{v \in V} N_{u,v}$) be the total number of messages stored at geographic location u in the initial state.

- Continuous workload model

  In continuous workload model, messages are continuously generated at every originating geographic location as a Poisson process. Let $\lambda_{u,v}$ be the message generation rate at originating geographic location u destined for geographic location v. Note that our analytic model is based on discrete random walks on a graph, so our analytic model itself is a discrete model. As we will explain in Section 2.3, our discrete model is linked with a continuous queueing model for approximately deriving the average message delivery delay.

2.3 Analysis

2.4 Single-Copy with One-Time Workload Model

We first consider the simplest case: single-copy geographic DTN routing (i.e., $C = 1$) with the one-time workload model. The average message delivery between any pair of geographic locations with any number M of mobile agents and any number K of message loadings is derived.

First, we focus on the case with the one-time workload model and a single mobile agent ($M = 1$).

It is well known that *hitting time*, which is the expected number of slots for mobile agent starting its random walk from vertex s to reach vertex t at

first, is given by the following equation [5].

$$H(s,t) = 2\,|E| \sum_{i=2}^{|V|} \frac{1}{1-\lambda_i} \left(\frac{v_{i,t}^2}{d(t)} - \frac{v_{i,s}\, v_{i,t}}{\sqrt{d(s)\, d(t)}} \right) \tag{1}$$

where λ_i and $v_{i,j}$ are i-th eigenvalue of $N = D^{1/2}\, A\, D^{1/2}$ ($\lambda_1 = 1 > \lambda_2, \ldots, \lambda_{|V|}$) and j-th element of i-th eigenvector corresponding to λ_i. D is the diagonal matrix with diagonal entries $1/d(1), \ldots, 1/d(|V|)$.

For delivery of a message from geographic location u to geographic location $v\,(v \neq u)$, the following three conditions must be satisfied: (1) the mobile agent starting its random walk at $k = 0$ arrives geographic location u, (2) a message destined for geographic location v is loaded (i.e., chosen by FIFO algorithm) by the mobile agent, and (3) the mobile agent delivers the message to geographic location v. Hence, the average massage delivery delay from geographic location u to geographic location v for $N_{u,v} \geq 1$ is given by

$$D_{u,v} \simeq H(s_m, u) + \sum_{n=1}^{\infty} p_{u,v}(n)\, (n-1)\, R_u + H(u,v), \tag{2}$$

where $p_{u,v}(n)$ is the probability that a message destined for geographic location v is loaded at the n-th visit of geographic location u. Also, R_u is the mean recurrence time at geographic location u (i.e., the expected number of slots between two successive arrivals of the mobile agent at geographic location u).

With FIFO algorithm, the mobile agent visiting at geographic location u moves (at most) the number K of messages randomly chosen from available messages at the buffer of geographic location u since freshness of all

available messages are identical. So, we have:

$$p_{u,v}(n) = \begin{cases} K/N_u & \text{if } n \leq N_u/K \\ \max(N_u - (n-1)\,K, 0)/N_u & \text{otherwise} \end{cases} \tag{3}$$

Since the visiting probability of the mobile agent at geographic location u is given by $\frac{d(u)}{2|E|}$, the mean recurrence time R_u is given by its reciprocal; i.e.,

$$R_u = \frac{2\,|E|}{d(u)}. \tag{4}$$

Second, we consider the case with the one-time workload model and multiple mobile agents ($M \geq 2$).

Let $H^M(\{s_1, \ldots, s_M\}, v)$ be the hitting time of multiple random walks (i.e., the expected number of slots for any of M mobile agents starting their independent discrete random walks from vertices $s_1, \ldots, s_M$ to reach vertex v at first). It is known that the hitting time of M random walks on graph G can be calculated from the hitting time of a single random walk on another graph $G^M = (V', E')$ [6]. $G^M = (V', E')$ is defined as

$$V' = \{(v_1, \ldots, v_M) | v_1, \ldots, v_M \in V\}, \tag{5}$$

$$E' = \{((u_1, \ldots, u_M), (v_1, \ldots, v_M)) | (u_1, v_1), \ldots, (u_M, v_M) \in E\}. \tag{6}$$

Let A_v ($\subset V'$) be the set of all vertices in G^M, which contain vertex $v \in V$.

$$A_v = \{(u_1, \ldots, u_M) | (u_1, \ldots, u_M) \in V', \exists i\ u_i = v\} \tag{7}$$

The hitting time of M random walks, $H^M(\{s_1, \ldots, s_M\}, v)$, is given by the time for a single random walk on G^M starting from vertex $(s_1, \ldots, s_M)$

to arrive at first any of vertices in A_v [6].

Hence, the average message delivery delay from geographic location u to geographic location v is given by

$$D_{u,v} \simeq H^M(\{s_1, \ldots, s_M\}, u) + \sum_{n=1}^{\infty} p_{u,v}(n)\,(n-1)\,R_u^M + H(u,v). \quad (8)$$

where R_u^M is the recurrence time of M mobile agents at geographic location u (i.e., the expected number of slots between two successive arrivals of any mobile agent at geographic location u). The recurrence time of M mobile agents, R_u^M, is equivalent to the average hitting time of a single random walk on G^M starting from vertex $v \in A_v$ and ending at $u \in A_v \setminus \{v\}$. Assuming a single random walk visits vertices in A_v with the equal probability, R_u^M is approximately given by

$$R_u^M \simeq \frac{\sum_{v \in A_u} H^M(v, A_u \setminus \{v\})}{|A_u|}, \quad (9)$$

where $H^M(v, S)$ is the time for a single random walk on G^M starting from vertex v to arrive at first any of vertices in S.

2.5 Single-Copy with Continuous Workload Model

We then consider a more generic case than that in Section 2.4: single-copy geographic DTN routing (i.e., $C = 1$) with the continuous workload model. Similar to the previous section, the average message delivery between any pair of geographic locations with any number M of mobile agents and any number K of message loadings is derived.

Note that we will consider more complex case — multiple-copy geographic DTN routing (i.e., $C \geq 2$) with the continuous workload model — in Section 2.6. Although the analysis presented in this section is a special

case of that in Section 2.6 where we will also derive the distribution of message delivery delays as well as the average message delivery delay. The advantage of the analysis in this section is computational efficiency; i.e., the analytic approach below is much more scalable than that in Section 2.6 in terms of the number of geographic locations and the number of mobile agents.

We focus on message arrivals and departures at geographic location u. A message generated at geographic location u and destined for geographic location v is awaited until it is loaded by a mobile agent visiting geographic location u. Since we consider geographic DTN routing with FIFO algorithm, messages generated at a geographic location are served in a FIFO-fashion. Once the message is loaded by a mobile agent visiting at geographic location u, the mobile agent keeps carrying the message until it arrives the geographic location v. Hence, the average message delivery delay from geographic location u to geographic location v, $D_{u,v}$, is given by the sum of *the average waiting time* in geographic location u until message loading and *the average delivery delay* between geographic locations u and v.

Let T_u be the average waiting time at geographic location u. Note that the waiting time are the same for all messages destined to different geographic locations since messages are loaded by mobile agents in a FIFO-fashion. The average delivery delay is simply given by the hitting time, $H(u, v)$. So, we have

$$D_{u,v} = T_u + H(u, v). \tag{10}$$

Since M mobile agents randomly walks on a graph, those M mobile agents randomly visit geographic location u. In other words, an arrival of

every mobile agent can be seen as a random process.

Here, we introduce a queueing model for deriving the average waiting time in geographic location u. Our analytic model is discrete since the mobility of mobile agents are modeled as multiple discrete random walks on a graph. When a slot length is sufficiently small, the dynamical process at geographic location u can be modeled by a continuous queueing model.

We assume that the interval between successive arrivals of a mobile agent at geographic location u is exponentially distributed with the mean of $1/\mu_u$. Note that M mobile agents move independently. So, arrival processes of those M mobile agents at geographic location u are also independent. Also note that in the continuous workload model, messages are generated as a Poisson process. For simplicity, we focus on the case of $K = 1$; i.e., only the oldest message is loaded by every mobile agent. Then, the arrival-and-departure process of messages at geographic location u can be approximated by $M/M/m$ queueing model (see Fig. 2).

So, the average waiting time at geographic location u is approximately given by the average waiting time of $M/M/m$ queueing model:

$$T_u \simeq \frac{1}{\mu_u} \left(1 + \frac{\tau_u}{M\,(1-\rho_u)} \right), \tag{11}$$

where

$$\rho_u \equiv \frac{\sum_{v \in V} \lambda_{u,v}}{M\,\mu_u}, \tag{12}$$

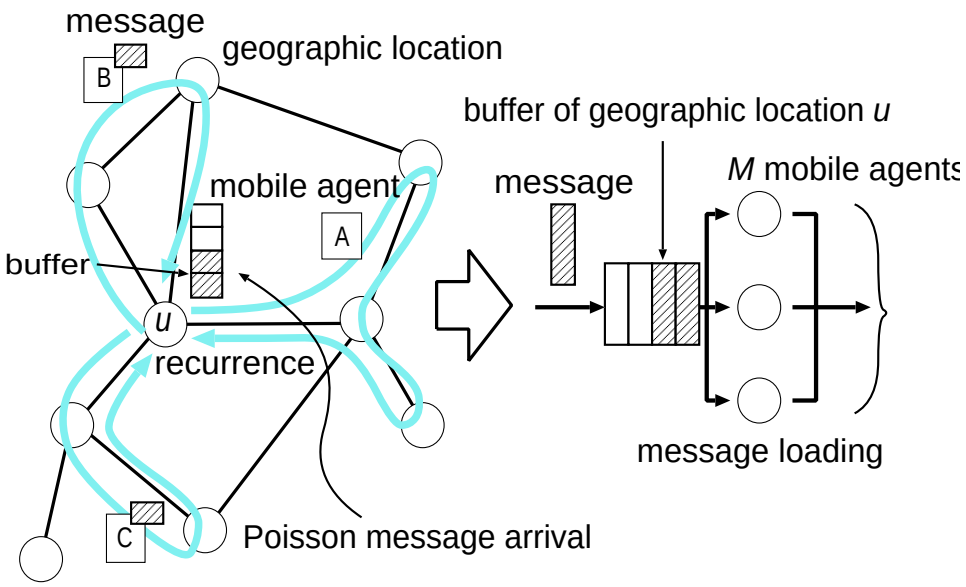

Figure 2: $M/M/m$ queueing model as a model of the arrival-and-departure process of messages at geographic location u

and

$$\tau_u = \frac{(M\,\rho_u)^M}{M!\,(1-\rho_u)}\,p_0, \tag{13}$$

$$p_0 = \left(1 + \frac{(M\,\rho_u)^M}{M!\,(1-\rho_u)} + \sum_{n=1}^{M-1}\frac{(M\,\rho_u)^n}{n!}\right)^{-1}. \tag{14}$$

The message loading rate of a mobile agent, μ_u, is given by the reciprocal of the average recurrence time, R_u, of a mobile agent (see Eq. 4). So, we have

$$\mu_u = \frac{1}{R_u}. \tag{15}$$

For $K \geq 2$, the average waiting time, T_u, can be approximated by re-

placing Eq. (15) with

$$\mu_u = \frac{K}{R_u}. \tag{16}$$

We note that this is just an approximation since the interval of successive departures with $K \geq 2$ is not exponentially distributed. We will examine the validity of our approximate analysis in Section 2.7.

2.6 Multiple-Copy with Continuous Workload Model

We consider a more generic case than previous cases: multiple-copy geographic DTN routing (i.e., $C \geq 2$) with the continuous workload model. In what follows, we derive the average and the distribution of message delivery delays between any pair of geographic locations with any number M of mobile agents and any number K of message loadings. Note that in a multiple-copy case, the message delivery delay is defined as the time elapsed until the *first delivery* among multiple replicas.

We focus on a message generated at originating geographic location u, which is destined for geographic location u. Let $c_1, c_2, \ldots, c_C$ be replicas of the message. The random variable representing the message delivery delay of replica c_i is denoted by X_i. The random variable representing the message delivery delay of replicas (i.e., $\min(X_1, X_2, \ldots, X_C)$) is denoted by X.

The average message delivery delay with replicas, $D_{u,v}$, is the expectation of message delivery delay. So we have

$$D_{u,v} = \sum_{k=1}^{\infty} k\, p_{u,v}(k), \tag{17}$$

where $p_{u,v}(k)\,(= P(X = k))$ is the probability that the message delivery

delay with replicas is k. $p_{u,v}(k)$ is given by its cumulative distribution function $P_{u,v}(k)$ as

$$p_{u,v}(k) = P_{u,v}(k) - P_{u,v}(k-1). \tag{18}$$

For simplicity, we assume that the number M of mobile agents is equal to the number C of replicas. We assume that every mobile agent loads at most a single replica for a specific message since loading multiple replicas simply wastes the network resources.

In this case, similarly to Section 2.5, the arrival-and-departure process of a replica at geographic location u can be approximated as $M/M/1$ queueing model (Fig. 3). The number M of mobile agents performs independent random walks on a graph, and under our assumptions, a mobile agent loads at most a single replica for a specific message at geographic location u.

Let $P^i_{u,v}(k)$ be the cumulative distribution function of $p^i_{u,v}(k)$ ($\equiv P(X_i = k)$). Since the message delivery delay of replicas, X, is the minimum of message delivery delays of all replicas, $X_1, X_2, \ldots, X_C$, we have

$$P_{u,v}(X = k) = 1 - \prod_{i=1}^{C}(1 - P^i_{u,v}(k)). \tag{19}$$

By definition, we have

$$P^i_{u,v}(k) = \sum_{l=1}^{k} p^i_{u,v}(l). \tag{20}$$

Naturally, if the message delivery delay of replica c_i is k, it means that the sum of the generation–loading time (i.e., the time awaited in the buffer of geographic location u) and the loading–delivery time (i.e., the time spent

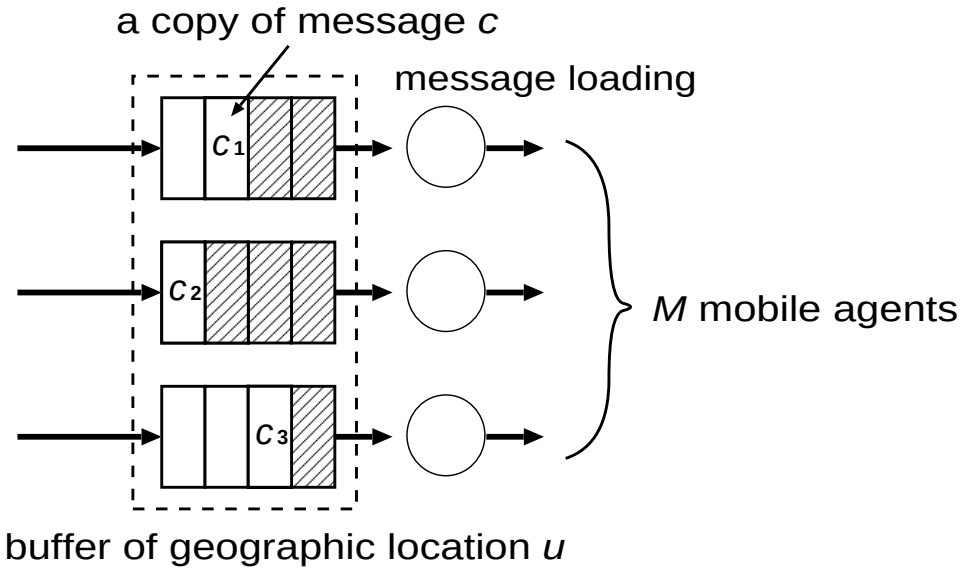

Figure 3: $M/M/1$ queueing model for multiple copies

by a mobile agent for message delivery is k). Thus, we have

$$p^i_{u,v}(k) = \sum_{l+n=k} p_T(l)\, p_D(n), \tag{21}$$

where $p_T(\cdot)$ and $p_D(\cdot)$ are the probability mass functions for the generation–loading time and the loading–delivery time, respectively.

The probability of seeing j unique messages at the time of message generation, $p_u(j)$, is simply given by the probability of having j customers in the buffer. Namely,

$$p_u(j) = \begin{cases} 1 - \rho_u^2 & j = 0 \\ 1 - \rho_u\, \rho^{j+1} & \text{otherwise} \end{cases} \tag{22}$$

where

$$\rho_u \equiv \frac{\sum_{v \in V} \lambda_{u,v}}{\mu_u}. \tag{23}$$

Let $p_T^j(k)$ be the conditional probability that the generation–loading time is k when the number j of unique messages already exist at the time of message generation. Then, we have

$$p_T(k) = \sum_{j=0}^{\infty} p_u(j)\, p_T^j(k). \tag{24}$$

Now we will derive the conditional probability $p_T^j(k)$. When j unique messages reside in the buffer at the time of replica c_i generation, replica c_i will be loaded at the $\lceil (j+1)/K \rceil$-th visit of the mobile agent at geographic location u. Let $q_u(k)$ be the probability that a mobile agent starting its random walk from anywhere on the graph visits geographic location u at first after k steps. Also, let $r_u(k)$ be the probability that a mobile agent starting its random walk from geographic location u revisits geographic location u exactly after k steps. Using $L_j \equiv \lceil (j+1)/K \rceil$, the conditional probability $p_T^j(k)$ is written as

$$p_T^j(k) = \begin{cases} q_u(k) & \text{if } L_j = 0 \\ \sum_{l_0+\cdots+l_{L_j}=k} q_u(l_0)\, r_u(l_1)\, r_u(l_2) \ldots r_u(l_{L_j}) & \text{otherwise} \end{cases} \tag{25}$$

Let $q_{u,v}(k)$ be the probability that a mobile agent starting its random walk from geographic location u visits geographic location v at first after k steps, $q_u(k)$ is given by

$$q_u(k) = \sum_{s \in V} \frac{d(s)}{2|E|}\, q_{s,u}(k). \tag{26}$$

Also, $r_u(k)$ is given by

$$r_u(k) = \sum_{u' \in V} q_{u,u'}(1)\, q_{u',u}(k-1). \tag{27}$$

Note that the hitting time distribution $q_{u,v}(k)$ is derived in [5].

2.7 Numerical Examples

We use two different types of network topologies for the following numerical examples: 3×3 grid topology (Fig. 4) and 9-node planar topology (Fig. 5).

Unless stated otherwise, we use three mobile agents ($M = 3$) and a single message loading ($K = 1$). Starting vertices of all mobile agents are set to vertex 1.

In the one-time workload model, every geographic location is placed with eight messages destined to all other geographic locations in the initial state. Namely, the total number of messages in the network is 72 ($= 9 \times (9 - 1)$).

2.8 Single-Copy with One-Time Workload Model

The distribution of average messages delivery delays with the one-time workload model in the grid topology is shown in Figs. 6 and 7. Each figure shows the effect of the number M of mobile agents (Fig. 6) and the effect of the number K of message loadings (Fig. 7). These figures show average message delivery delays of all geographic location pairs obtained from our approximate analysis (solid line) and simulations (dotted line). Simulation results are the average of measurements obtained with 10,000 simulation runs. Numerical results and simulation results for the 9-node planar topology is shown in Figs. 8 and 9.

Since both network topologies have nine geographic locations, the number of distinct geographic location pairs is 72. We measure average messages delivery delays for all pairs, and those values are sorted in ascending

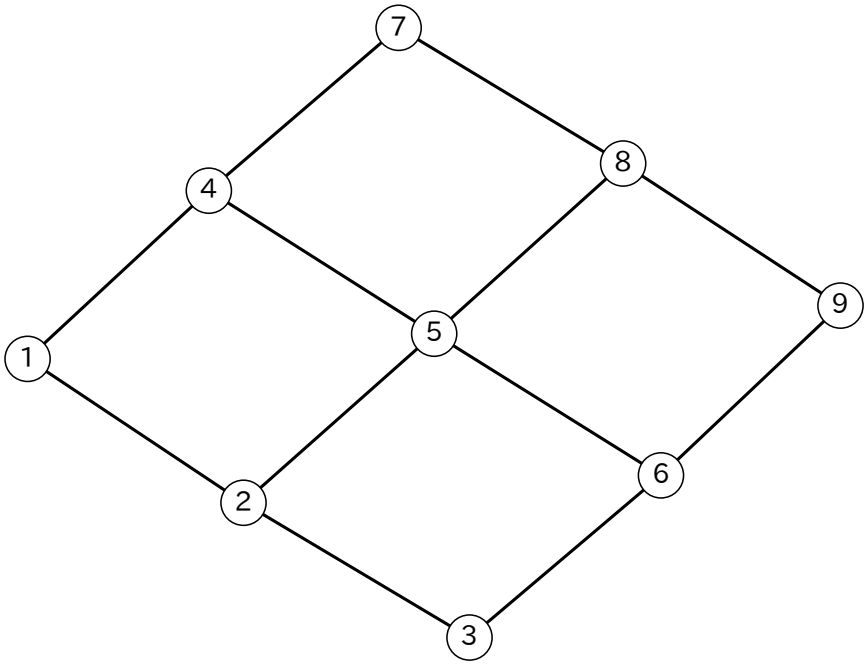

Figure 4: 3×3 grid topology

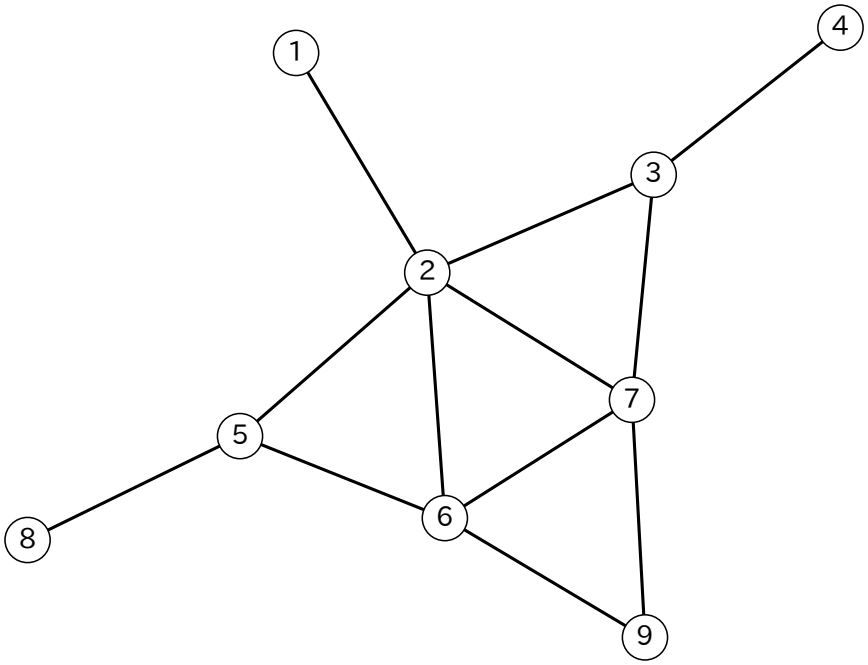

Figure 5: 9-node planar topology

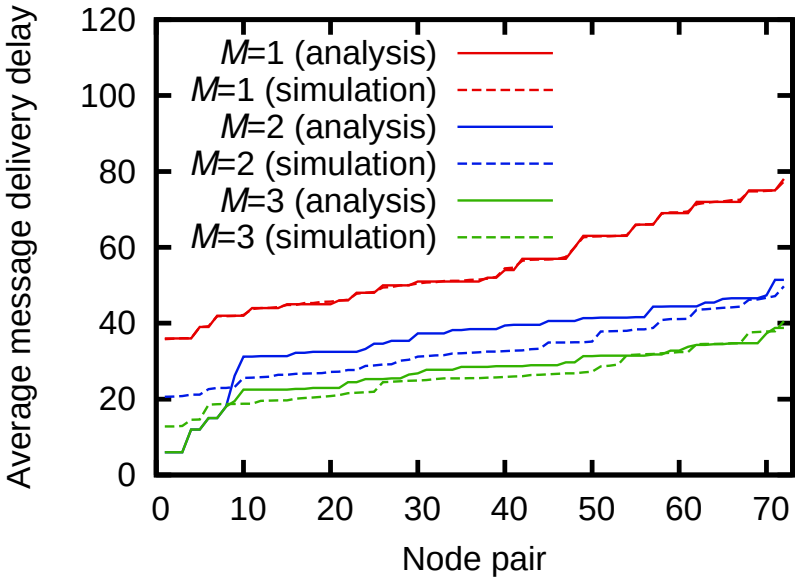

Figure 6: Effect of the number M of mobile agents (average message delivery delay in 3×3 grid topology with one-time workload model)

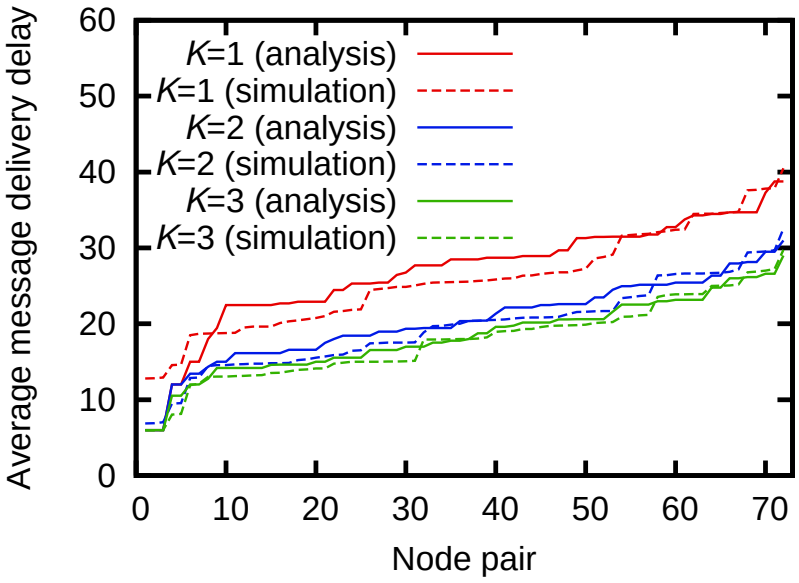

Figure 7: Effect of the number K of message loadings (average message delivery delay in 3×3 grid topology with one-time workload model)

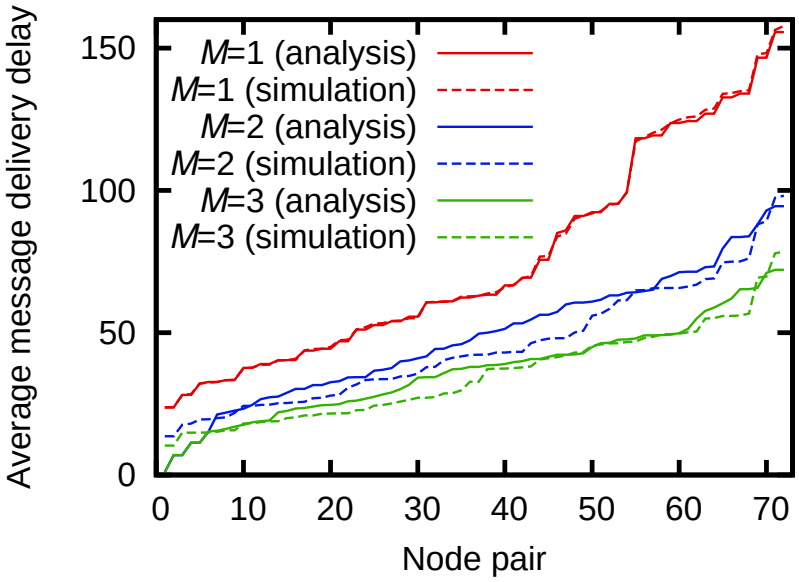

Figure 8: Effect of the number M of mobile agents (average message delivery delay in 9-node planar topology with one-time workload model)

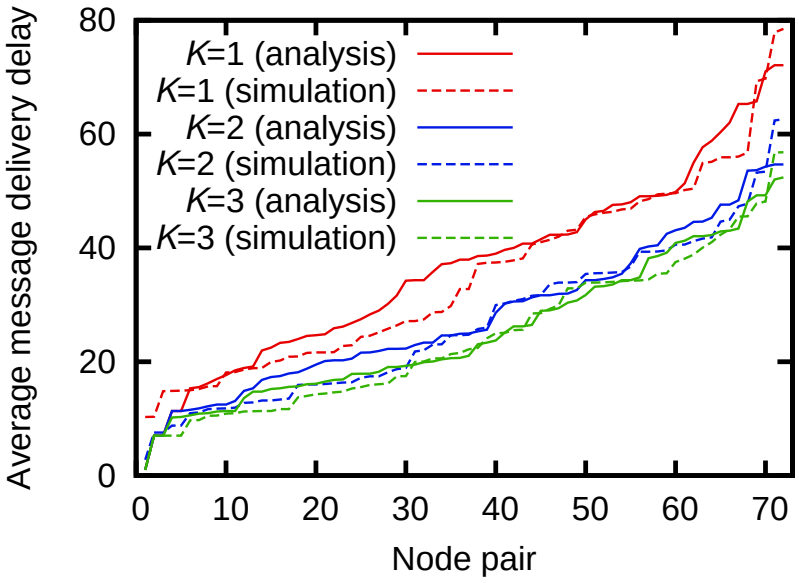

Figure 9: Effect of the number K of message loadings (average message delivery delay in 9-node planar topology with one-time workload model)

order. Thus, the average message delivery delays of node pair 1 and node pair 72 in Figs. 6 and 7 are the minimum and the maximum average message delivery delays among all geographic location pairs.

Comparison of Figs. 6, 7 and 8, 9 tells that the network topology has a strong impact on the average message delivery delay. In the 9-node planar topology, the average message delivery delays range more widely than in the grid topology. The rapidity of message delivery is significantly affected by the locations of originating and destination geographic locations. Our approximate analysis quantitatively levels how the average message delivery delay is affected by the network topology.

One can find from Figs. 6 and 8 that increasing the number M of mobile agents speeds up the message delivery, but the performance improvement is not uniform among geographic location pairs. Namely, the larger number of mobile agents are more beneficial to geographic location pairs with larger average message delivery delays. On the other hand, contrary to one's expectation, Figs. 7 and 9 indicates that increasing the number K of message loadings is not so significant. Increasing the number M of mobile agents and increasing the number K of message loadings should have similar impact since both increases the chance of message loading at originating geographic locations. However, these two factors have quite different impact of the average message delivery delay.

Also, one can find from these figures that our approximate analysis successfully capture the characteristics of geographic DTN routing with the FIFO algorithm. Our numerical results and simulation results generally coincide.

2.9 Single-Copy with Continuous Workload Model

The distribution of average messages delivery delays with the continuous workload model in the grid topology is shown in Figs. 10 and 11. Also, results in the 9-node planar topology is shown in Figs. 12 and 13. In Figs. 10 and 12, message generation rates are set to $\lambda_{u,v} = 0.01$ and $\lambda_{u,v} = 0.005$, respectively so that the network is lightly congested. We note that our approximate analysis is to understand the characteristics of the message delivery delay under, in particular, high traffic load.

One can find from these figures that the average message delivery delay diverges when the number M of mobile agents is small (i.e., $M = 1$) or message generation rate $\lambda_{u,v}$ is large. This is simply because with the continuous workload model, different from that the one-time workload model, the number of messages awaited in the buffer of a geographic location might continuously increase if the message loading is slower than the message generation. Our approximate analysis is therefore useful to quantify the *effective capacity* of the geographic DTN routing.

Comparison of numerical results and simulation results indicates our approximate analysis well explains the impact of the number M of mobile agents and the message generation rate $\lambda_{u,v}$. In particular, the saturating point (i.e., the node pair at which the average message delivery delay diverges) in numerical results and simulation results almost perfectly agree. On the contrary, modest discrepancy between numerical results and simulation results when the message generation rate is rather low. More detailed investigation would be approximate to further improve the accuracy of our approximate analysis.

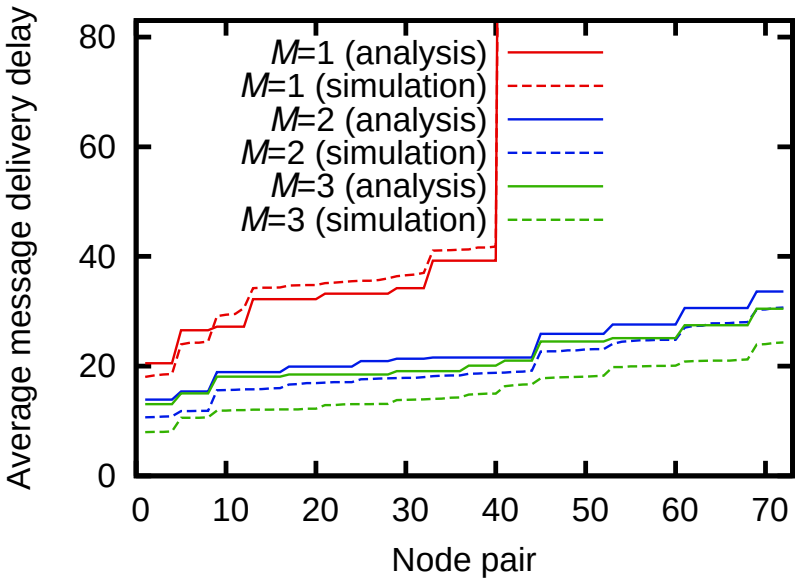

Figure 10: Effect of the number M of mobile agents ($\lambda_{u,v} = 0.01$) (average message delivery delay in 3×3 grid topology with continuous workload model)

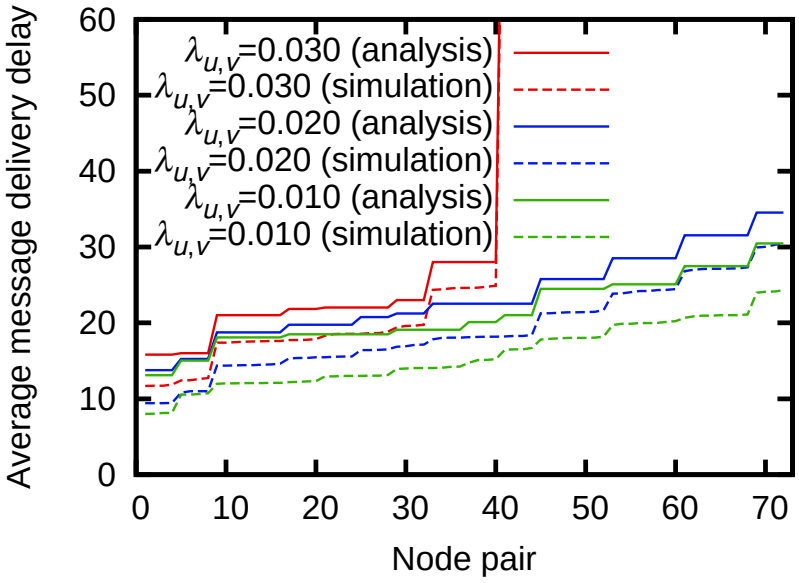

Figure 11: Effect of message generation rate (average message delivery delay in 3×3 grid topology with continuous workload model)

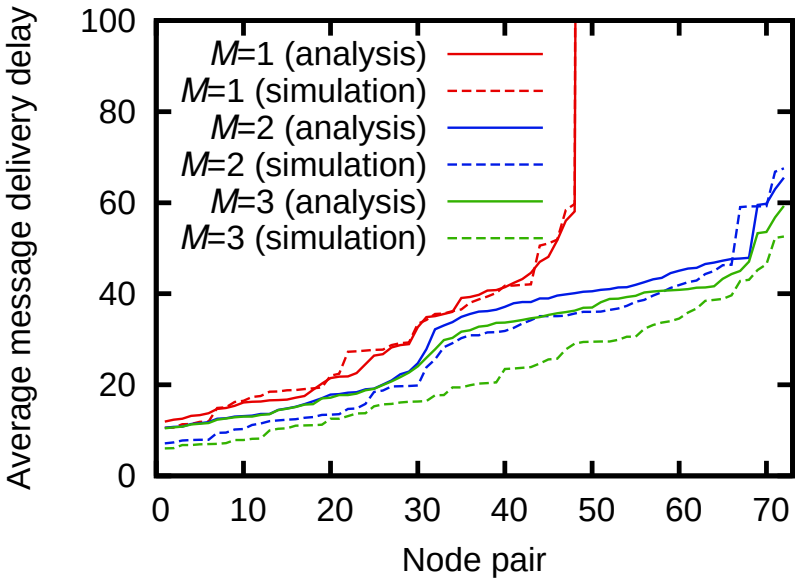

Figure 12: Effect of the number M of mobile agents ($\lambda_{u,v} = 0.01$) (average message delivery delay in 9-node planar topology with continuous workload model)

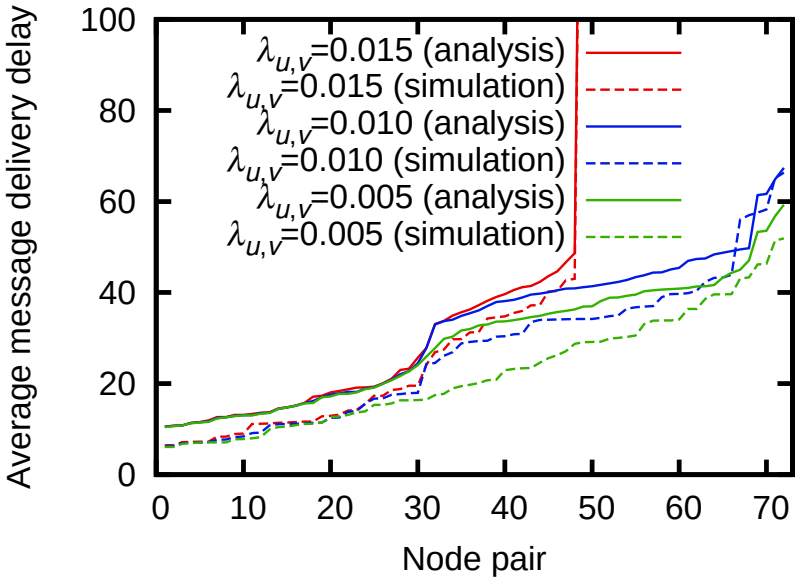

Figure 13: Effect of message generation rate (average message delivery delay in 9-node planar topology with continuous workload model)

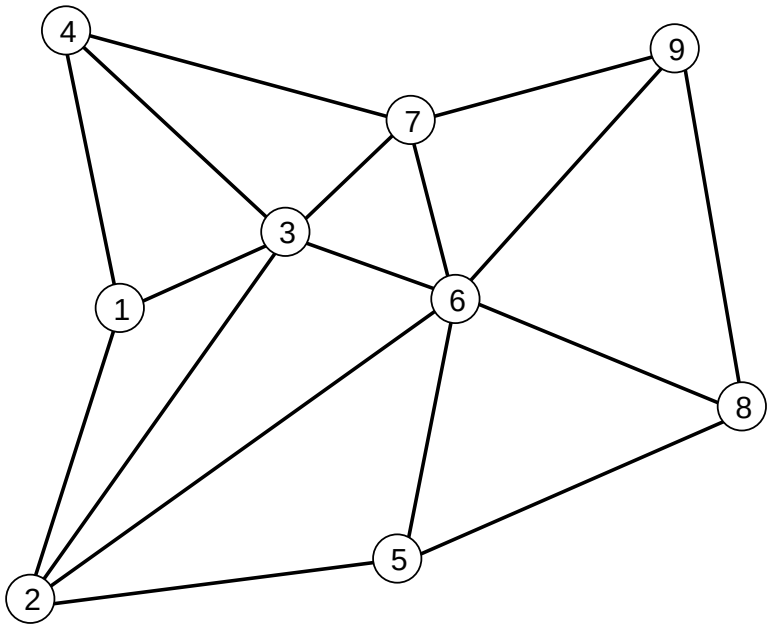

Figure 14: 9-node triangle topology

2.10 Multiple-Copy with Continuous Workload Model

We investigate how the number C of message replicas affects the average message delivery delay and the distribution of message delivery delays through several numerical examples. Moreover, we examine the validity of our analysis by comparing numerical results with simulation results.

The average message delivery delays of all geographic location pairs are shown in Fig. 15. The distribution of relative errors in the average message delivery delay is shown in Fig. 16. The network topology we used to calculate numerical examples is shown in Fig. 14. The distribution of the message delivery delays is shown in Figs. 17 and 18. In Figs. 15, 16, 17 and 18, the message generation rate is set to $\lambda_{u,v} = 0.005$. Also, the number of message loadings is set to $K = 1$ and the number C of message replicas is changed to 2, 4 and 8.

Figure 15 shows that our analysis can explain the difference in delays

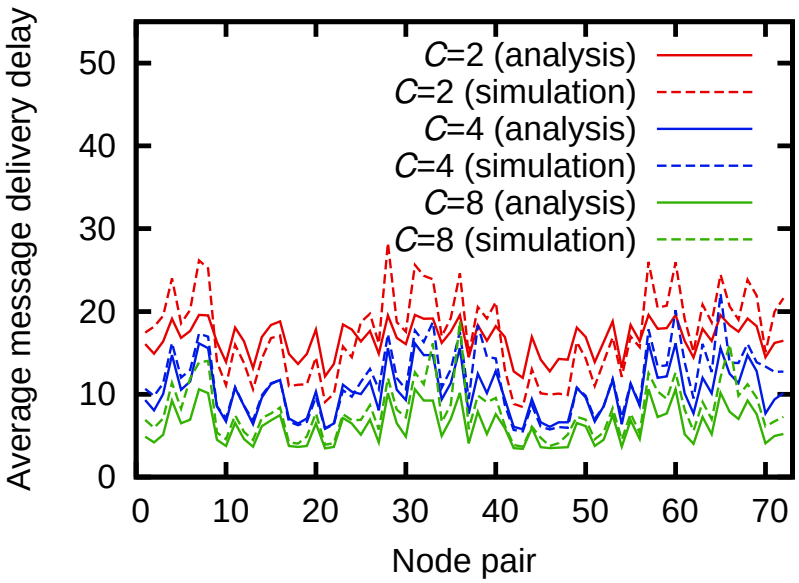

Figure 15: Average message delivery delay in 9-node triangle topology with continuous workload model (multiple-copy)

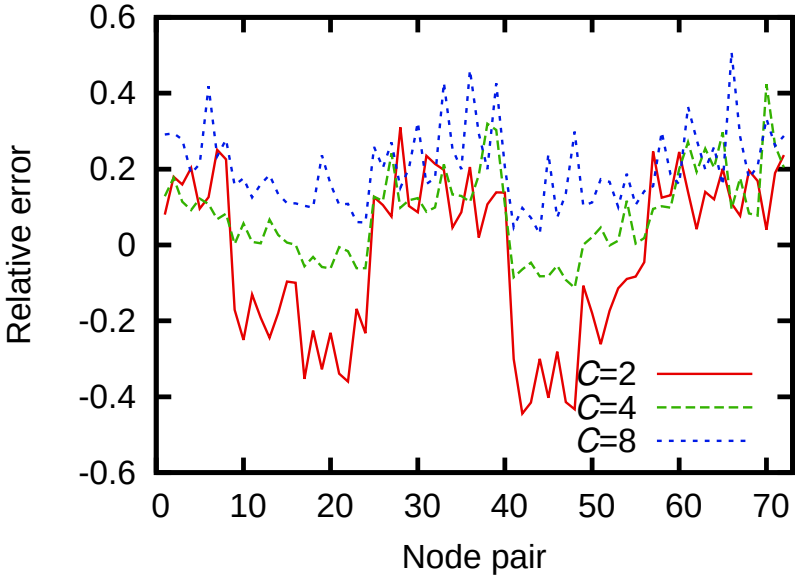

Figure 16: Relative error of the average message delivery delay

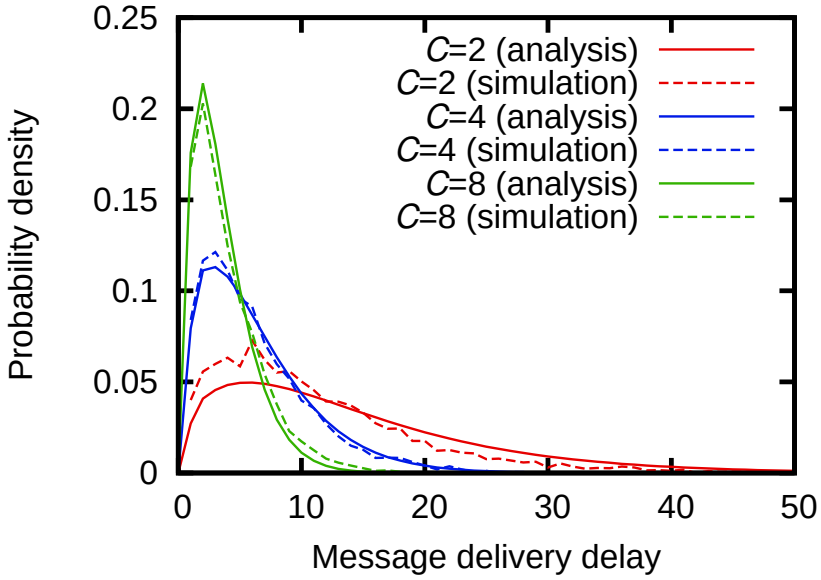

Figure 17: Distribution of message delivery delays from geographic location 3 to geographic location 2

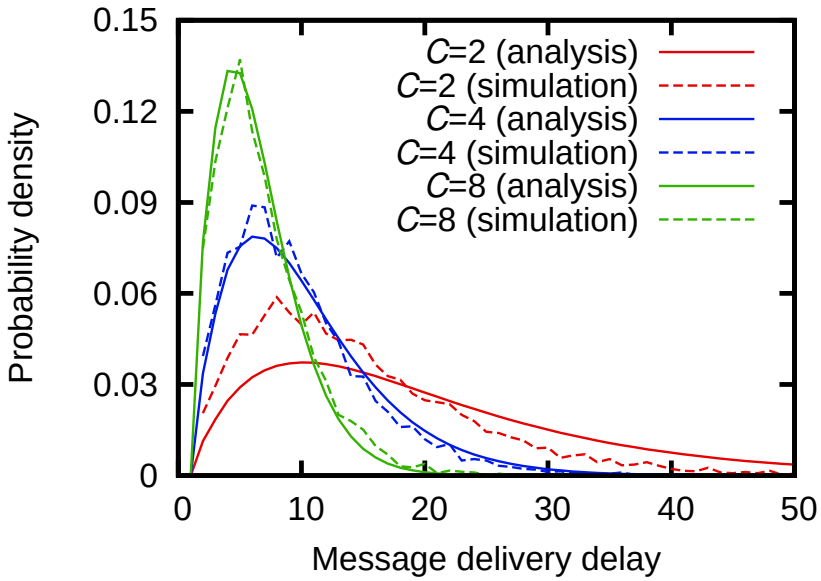

Figure 18: Distribution of message delivery delays from geographic location 3 to geographic location 9

among geographic locations, and the numerical examples are generally smaller than the simulation results. Also, it can be seen from these figures that the average message delivery delay decreases as the number C of message replicas increases.

2.11 Case Study

Utilizing our analysis results, we discuss a possible application of geographic DTN routing — communication among evacuation sites in disaster area.

Large-scale disasters such as earthquakes, hurricanes and tsunamis may severely damage our network infrastructure [7]. In the large-scale earthquake occurred in the northern area of Japan in 2011, it has been reported that the mobile cellular networks and electrical/optical Internet infrastructure had been disconnected for more than couple weeks at several areas.

In such disaster areas, people stay at one of nearby evacuation sites for safety reasons. Provision of communication among those refugees are strongly required [8]. People at an evacuation site should be able to communicate with their family, relatives and friends who might be at other evacuation sites. They should be able to receive information from external information sources including governments and local communities.

A geographic DTN routing can be a viable solution for providing communications among people in evacuation sites. People may carry battery-powered smartphones and/or tablets, which have adhoc wireless communication capability. Those portable devices can be utilized to build adhoc networking infrastructure [9, 10]. In particular, people are tend to stay closer at evacuation sites, and those evacuation sites are fixed. So, if we regard evacuation sites as *geographic locations* and people moving across

evacuation sites with their smartphones and/or tablets as *mobile agents*, geographic DTN routing can be realized.

The fundamental question on such geographic DTN routing among evacuation sites in disaster area is its feasibility. For instance, it is unclear how many mobile agents (i.e., people carry smartphones and/or tablets) are required to realize communication among evacuation sites without dedicated networking infrastructures. We therefore utilize our analysis results to investigate the above question.

As an example, we use the placement of evacuation sites shown in Fig. 14, which illustrates, for instance, nine evacuation sites (e.g., elementary/high schools in Japan) at a small town. The links connecting evacuation sites are paths (e.g., roads). Let M be the number of people participating the geographic DTN routing. We assume the random walk mobility for all participants (i.e., mobile agents). For simplicity, we assume a heterogeneous discrete random walks for all participants; i.e., every participant randomly moves to one of neighbor evacuation sites with the identical probabilities at every slot. The slot length is assumed to be 30 minutes; i.e., a participant spends 30 minutes in total for movement to and staying in a neighbor evacuation site.

Figure 19 shows the average message delivery delay between evacuation sites under different load factors. Load factor ρ is defined as $\rho = \lambda_u/\mu_u$. λ_u is the message generation rate at evacuation site u (i.e., $\lambda_u = \sum_{v \in V} \lambda_{u,v}$). μ_u is the message loading rate of a mobile agent at evacuation site u (i.e., $\mu_u = \frac{1}{R_u}$).

This figure clearly shows the average message delivery delay is significantly reduced as the number of mobile agents increases, in particular, when the load factor ρ is high. This figure implies that, for instance, the

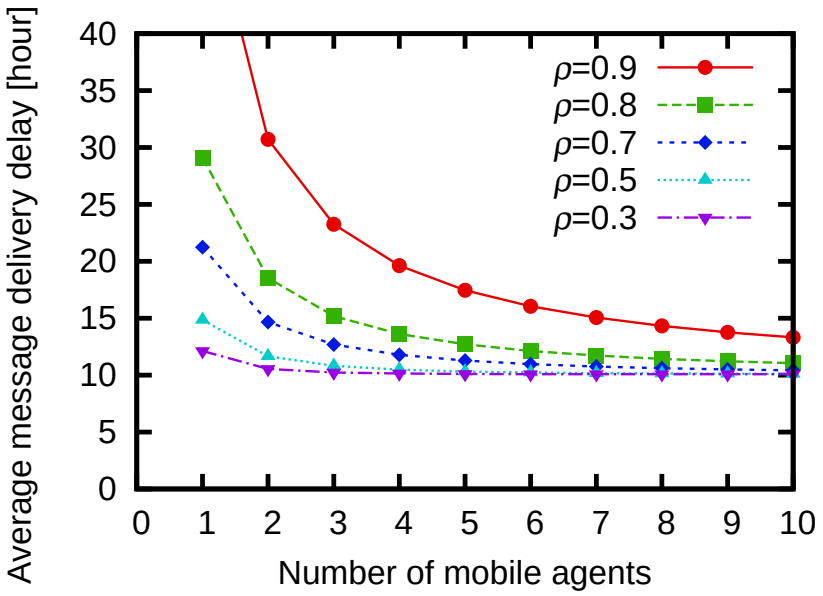

Figure 19: Average message delivery delay among evacuation sites

message delivery within 12 hours could be realized only with geographic DTN routing among people carrying smartphones and/or tables when the message generation rate is modest and/or a sufficient number of people is participated in geographic DTN routing.

2.12 Conclusion

In this section, we have derived the average message delivery delay in geographic DTN routing with the FIFO algorithm under one-time workload model and continuous workload model. We have modeled the behaviors of mobile agents as multiple random walks on a graph. We have analyzed the effect of system parameters — the number M of mobile agents on the field, the number K of message loadings at a geographic location, the message generation rate $\lambda_{u,v}$ and the number C of message replicas — on the average message delivery delay. We also have discussed the feasibility of a specific application of geographic DTN routing — communication among

evacuation sites in disaster area.

Our future work includes extensive simulations under realistic scenarios to further validate our approximate analysis, and extension of our analysis to incorporate more realistic geographic DTN routing such as geometry-aware routing algorithms, and other mobility patterns than the random walk.

3 Analysis of Message Delivery Delay in Large-Scale Geographic DTN Routing

In this section, we address the following research questions.

1. *How well or badly does geographic DTN routing perform in a large-scale network (i.e., a network with many geographic locations)?*

   A fundamental question on geographic DTN routing is whether it is scalable in terms of the number of nodes (geographic locations). Note that, in this section, a *network* means a network of geographic locations, each of which is generally connected with other geographic locations, rather than a network of mobile agents as in conventional DTN routing. A large-scale network therefore means a network with a large number of geographic locations.

   Our previous works [4, 11] investigate the feasibility of geographic DTN routing in rather small-scale networks because of computational complexity of geographic DTN routing simulations and analytical intractability of geographic DTN routing.

   Intuitively, the larger the network becomes, the lower the performance of geographic DTN routing becomes since the mobile agent is less

likely to arrive at the originating node as well as the destination node. However, it is unclear how quantitatively the performance of geographic DTN routing degrades as the number of geographic locations increases. Understanding the scalability of geographic DTN routing is crucial to design a geographic DTN routing protocol satisfying performance requirements.

2. *How is the performance of geographic DTN routing affected by the topology of the network (i.e., connections of many geographic locations)?*

   Another question is on the impact of the network topology on the performance of geographic DTN routing. In this section, a *network* means a network of geographic locations and the *topology* means the topology of the network composed of geographic locations and connections among them. The performance of geographic DTN routing should be affected by several factors: a geographic DTN routing algorithm, a buffer management mechanism of mobile agents, the capability (e.g., bandwidth and BER (Bit Error Ratio)) of wireless communication among mobile agents and geographic locations, the mobility of mobile agents, and the topology of geographic locations. Among those, the first four factors are *controllable* to some extent. For instance, the capability of wireless communication among mobile agents and geographic locations can be changed by replacing communication protocols and adjusting wireless device parameters. On the other hand, the last two factors are generally *uncontrollable*. It is generally difficult or impossible, for instance, to force mobile agents a specific mobility and/or to change the topology of geographic locations, which usually requires replacement of geographic locations and/or reconstruction of paths among geographic locations. Hence,

it is quite important to understand the impact of the network topology on the performance of geographic DTN routing.

In the literature, the impact of the network topology on conventional DTN routing has been investigated [12]. These studies show that the performance of conventional DTN routing is dependent on the underlying network topology. Also, in the field of network science, the relation between the topological structure of a complex graph and its dynamical properties such as the percolation, epidemics, and information dissemination has been extensively studied [13, 14]. These studies show that the network topology considerably affects the dynamical properties such as a probabilistic information dissemination on a complex network. By taking account of these findings, it is natural to assume that the performance of geographic DTN routing should be significantly affected by the network topology since geographic DTN routing has similarity with conventional DTN routing and dynamical processes on a complex network. However, the impact of the network topology on geographic DTN routing has not been well understood.

To the best of our knowledge, one exception is our previous work [11], in which the average and the distribution of message delivery delays are derived. However, as we have explained above, the analytical approach presented in [11] lacks scalability in terms of the network size, which makes it difficult to investigate the impact of the network topology on the performance of geographic DTN routing in medium-scale and large-scale networks.

In this section, we try to answer the above two questions by extending our previous work — a hybrid modeling of geographic DTN routing [11]

— with the help of recent advancement in analytical studies of random walks on a graph. In [11], a hybrid model of geographic DTN routing under random walk mobility on an arbitrary network topology is presented and the major performance metrics of geographic DTN routing such as the average and the distribution of message delivery delays are derived. The key idea in [11] is to combine a continuous-time model (i.e., an $M/M/1$ queueing model) and a discrete-time model (i.e., a discrete multiple random walks on a graph) to model the series of message delivery processes in geographic DTN routing. However, the analytical approach in [11] lacks scalability; the computational complexity to obtain numerical results in [11] grows exponentially as the network size (i.e., the number of geographic locations) increases. So, the analytical approach pin [11] is not applicable to answer the above two questions.

The major contributions of this section are summarized as follows.

- We present a hybrid model of multiple-copy geographic DTN routing, which is composed of a continuous $M/M/1/PS$ queueing model and discrete multiple random walks on a large-scale network
- We approximately derive the average message delivery delay in geographic DTN routing under random walk mobility on a large-scale network
- We analytically obtain the optimal number of message replicas (i.e., the number of copies per a message)
- We show that geographic DTN routing is scalable; i.e., its average message delivery delay is approximately proportional to the network size (i.e., geographic locations) unless heavily loaded

- We show that the network topology has *limited* impact on the performance of geographic DTN routing except heavily loaded conditions; the average message delivery delay is mostly determined by the degree of the destination node

3.1 Analytic Model

This subsection presents our analytic model used throughout this section

We model the field comprising of multiple geographic locations and paths connecting those geographic locations as an undirected graph $G = (V, E)$ where vertices and edges correspond to geographic locations and paths, respectively. Let $d(v)$ be the degree of vertex $v \in V$.

We model the behavior of a mobile agent in geographic DTN routing as a discrete random walk on graph G. At every slot, a mobile agent randomly and synchronously moves one of its neighbor vertices in G. Namely, a mobile agent on vertex v at slot k randomly moves to one of neighbor vertices with probability $1/d(v)$ at slot $k + 1$.

Note that the random walk mobility model is one of the most popular random mobility models in DTN performance studies because of its simplicity and tractability [15]. The random walk mobility model is based on the observation that mobile nodes naturally move around in unpredictable ways [15].

Every mobile agent performs message delivery using FIFO algorithm. When a mobile agent visits a geographic location, it performs the following operations: (1) moves at most K oldest messages from geographic location's buffer to mobile agent's buffer (message loading), and (2) moves, if any, all messages destined for the current geographic location from mobile agent's buffer to geographic location's buffer. The freshness of a message

is simply determined by the age of the message (i.e., the time elapsed since the time of its generation). In message loading, if there exist multiple messages of the same freshness, any of those messages are randomly selected. In our analysis, it is assumed that the buffer of geographic locations and mobile agents are sufficiently large.

In this chapter, we focus on geographic DTN routing with the number M of mobile agents.

There exist two classes of geographic DTN routing: *single-copy* and *multiple-copy*. In the single-copy case, every message is not duplicated in the network. So, a single-copy geographic DTN routing consumes least network resources. However, message delivery delays in the single-copy case tend to be large, and the message delivery probability from the originating node to the destination node is generally low. For accelerating message delivery and increasing the likelihood of message delivery, a message is duplicated in the multiple-copy case. In this section, the number of replicas for a message generated at originating geographic location u and destined for geographic location v is denoted by $C_{u,v}$.

We assume that messages are continuously generated at every originating geographic location as a Poisson process. Let $\lambda_{u,v}$ be the message generation rate at originating geographic location u destined for geographic location v. A single message consists of the number $C_{u,v}$ of message replicas. Note that our analytic model is based on discrete random walks on a graph, so our analytic model itself is a discrete model [11].

3.2 Derivation of Average Message Delivery Delay

In what follows, the average message delivery delay of multiple-copy geographic DTN routing under random walk mobility in a large-scale net-

work.

We focus on message m generated at originating node u and destined for destination node v. For brevity, $C_{u,v}$ is denoted as C; i.e., $C_{u,v}$ and C are used interchangeably. Let $r_1, r_2, \ldots, r_C$ be replicas of message m. In the multiple-copy case, the message delivery delay is defined as the time elapsed since message m is generated at originating node u until one of replicas $r_1, \ldots, r_C$ arrives at destination node v at first.

Let X_i be the random variable representing the delivery delay of replica r_i, which is defined as the duration between the message generation at the originating node and the arrival of replica r_i at the destination node. Also, let X be the random variable representing the message delivery delay. By definition, we have

$$X = \min(X_1, X_2, \ldots, X_C). \tag{28}$$

Hence, the cumulative distribution function of message delivery delay X, $F(X)$, is given by

$$F(x) = 1 - \prod_{i=1}^{C}(1 - F_i(x)), \tag{29}$$

where $F_i(x)$ is the cumulative distribution function of replica delivery delay X_i. The average message delivery delay of message m, $D_{u,v}$, is given by

$$D_{u,v} \equiv E[X] = \int_0^\infty x\, f(x)dx, \tag{30}$$

where $f(x)$ is the probability density function of message delivery delay X (i.e., $f(x) \equiv dF(x)/dx$).

Now we need to derive the cumulative distribution function of replica delivery delay X_i, $F_i(x)$.

The delivery delay of replica r_i is composed of the queueing delay at originating node u and the transfer delay from originating node u to destination node v. More specifically, the delivery delay of replica r_i is the sum of (1) the time elapsed from the generation of message m consisting of all replicas until loading of replica r_i by a mobile agent visiting originating node u (queueing delay), and (2) the time elapsed from the departure of the mobile agent carrying replica r_i until its arrival at destination node v (transfer delay). Random variables representing the queueing delay and the transfer delay of replica r_i are denoted by X_i^Q and X_i^T, respectively. Thus,

$$X_i = X_i^Q + X_i^T. \tag{31}$$

For simplicity, we use the following approximation.

$$X_i \simeq E[X_i^Q] + X_i^T. \tag{32}$$

We then introduce our hybrid model composed of a continuous $M/M/1/PS$ queueing model and discrete multiple random walks on a large-scale network.

First, the departure process from originating node u is modeled as an $M/M/1/PS$ queueing model where messages and loading by a mobile agent in geographic DTN routing correspond to customers and the service in the $M/M/1/PS$ queueing model. Namely, every message, which is composed of the number C of replicas, is regarded as a customer. Once the message (i.e., customer) is generated, it is added to the buffer of origi-

nating node u. We assume that when a mobile agent arrives at originating node u, it loads the number K of replicas among all messages queued from originating node's buffer in a round-robin fashion.

Provided that replicas $r_1, r_2, \ldots, r_C$ are processed sequentially and that the departure process from the originating node is stationary, the average queueing delay of replica r_i is approximately given by

$$E[X_i^Q] \simeq \frac{i}{C} E[X_C^Q]. \tag{33}$$

The average queueing delay of the last replica, r_C, is given by the average response time of the $M/M/1/PS$ queueing model:

$$E[X_C^Q] = \frac{1/\mu_u}{1 - \lambda_u/\mu_u}, \tag{34}$$

where λ_u and μ_u are the arrival rate and the service rate of the $M/M/1/PS$ queueing model, respectively. The arrival rate λ_u at originating node u is given by the sum of all message generation rates.

$$\lambda_u = \sum_{v \in V, v \neq u} \lambda_{u,v} \tag{35}$$

Recall that a mobile agent can load at most K replicas at every visit at the originating node. Also recall that every customer (i.e., message) is composed of C replicas. Thus, message m needs C times loading of replicas by mobile agents visiting originating node u. The service rate at originating node u is therefore approximately given by

$$\mu_u \simeq \frac{M\,K}{R_u\,C}, \tag{36}$$

where R_u is the average recurrence time of a mobile agent at originating node u, which is given by the following equation [5].

$$R_u = \frac{2\,|E|}{d(u)} \tag{37}$$

Second, the message transfer with multiple replicas from originating node u to destination node v is modeled as discrete multiple random walks on graph G. All replicas of message m, $r_1, r_2, \ldots, r_C$ are sequentially loaded by different mobile agents visiting at originating node u.

It is shown in [16] that the average hitting time $H_{u,v}$ of a random walk on sufficiently large and reasonably connected graph G starting from vertex u and ending at vertex v is approximately given by

$$H_{u,v} \simeq \frac{2\,|E|}{d(u)}. \tag{38}$$

Assuming that hitting times of a random walk on graph G is exponentially distributed, the probability density function of replica delivery delay X_i is given by the $E[X_i^Q]$-*shifted* exponential distribution with the mean of $H_{u,v}$. For brevity, let Δ be $E[X_i^Q]$.

$$f_i(x) = \begin{cases} \frac{1}{\Delta + H_{u,v}}\, e^{-\frac{x-\Delta}{\Delta+H_{u,v}}} & x \geq \Delta \\ 0 & \text{otherwise} \end{cases} \tag{39}$$

Finally, integration of the probability density function $f_i(x)$ yields

$$F_i(x) = 1 - e^{-\frac{x-\Delta}{\Delta+H_{u,v}}}. \tag{40}$$

3.3 Notes on Optimal Number of Message Replicas

In this subsection, we analytically obtain the optimal number of message replicas that minimizes the average message delivery delay.

As we will show in Section 2.7, the optimal number of message replicas in terms of the average message delivery delay is dependent on several system parameters. Among several system parameters, the number of message replicas is easier to change than others such as the number of geographic locations, the topology of the network, and the number of mobile agents. In other words, geographic DTN routing algorithms can dynamically change the number of message replicas to optimize its performance.

One possible application of our approximate analysis is to optimize the number of message replicas at every originating node based on its observations. The optimal number $C^*_{u,v}$ of message replicas for messages originated at geographic location u and destined for geographic location v can be easily obtained by numerically solving the following equation.

$$C^*_{u,v} = \underset{1 \le C \le M}{\operatorname{argmin}} D_{u,v} \tag{41}$$

Implementation of such an optimization mechanism in a geographic DTN routing algorithm is not difficult; necessary information for originating node u to obtain the optimal number C^* of message replicas are message generation rate $\lambda_{u,v}$, the maximum number K of message loadings, the number M of mobile agents, the number $|E|$ of edges (i.e., paths) in the network, and the degree $d(v)$ of the destination node. Every geographic location knows the first two, and others are not difficult to obtain or estimate because those are generally not dynamically varying.

3.4 Numerical Examples and Discussion

In this section, we present several numerical examples to investigate the scalability of geographic DTN routing as well as the impact of the network topology on its performance. Simulation results are also provided to validate our approximate analysis.

For a given network size $N\,(=|V|)$ (i.e., the number of geographic locations), a network topology is synthetically generated using ER (Erdös-Rényi) model [17]. The average degree (i.e., the average number of paths connected to a geographic location) $\overline{k}$ is fixed at $\overline{k} = 6$. Hence, the total number of edges among geographic locations are $|E| = \overline{k}\,N/2 = 3\,N$.

With network topology G of size N, the number of possible originating and destination (i.e., source and sink) node pairs is too many (i.e., N^2) to examine every pair. So, in our experiments, we choose both originating and destination nodes from graph G according to the following rules.

1. The originating node u is set to the node with the largest degree in graph G, which corresponds to the *hub* geographic location in the network.

2. The destination node v is randomly chosen from nodes whose degree is exactly k, which corresponds to a *typical* geographic location in the network.

Note that in our experiments, only a single originating-and-destination node pair is examined.

The message generation rate $\lambda_{u,v}$ has different meanings under different conditions. For instance, if the number M of mobile agents is small and/or the network size N is large, mobile agents are not likely to visit an originating node, resulting in high offered load. For enabling comparison

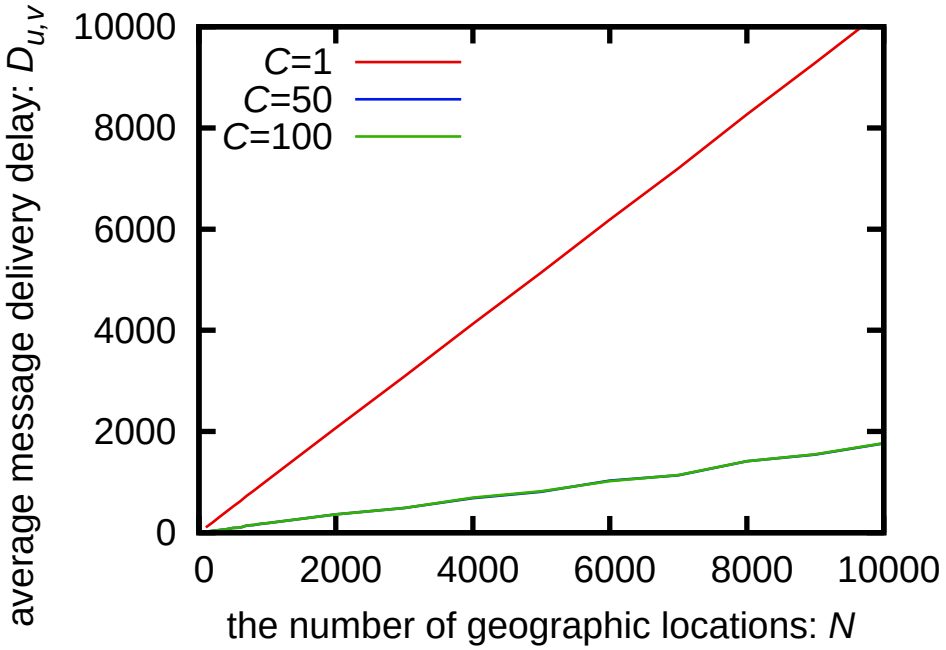

Figure 20: Relation between the number N of geographic locations and average message delivery delay $D_{u,v}$.

of numerical results under different system parameters, the message generation rate $\lambda_{u,v}$ is normalized using a load factor α $(0 \leq \alpha \leq 1)$ as $\lambda_{u,v} = \alpha\, \mu_u$ (see Eq. 36).

Unless stated otherwise, the following system parameters are used: network size (the number of geographic locations) $N = 1,000$, the number of mobile agents $M = 100$, the number of message replicas $C_{u,v} = C = 1$ for all originating and destination node pairs, load factor $\alpha = 0.8$ (i.e., modestly-loaded condition), and the maximum number of message loadings $K = 1$.

Figure 20 shows the average message delivery delay $D_{u,v}$ for different network sizes N. In this figure, the number C of message replicas is changed to 1, 50, or 100. Note that results with $C = 50$ and $C = 100$ (blue and green line) are almost indistinguishable.

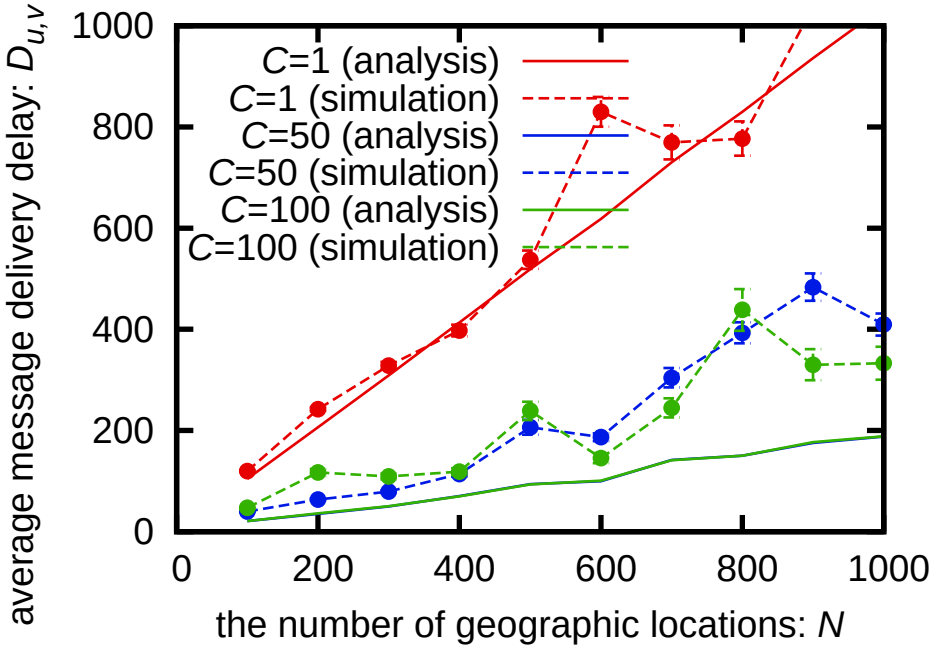

Figure 21: Comparison of numerical results and simulation results.

Comparison of numerical examples and simulation results is plotted in Fig. 21. Due to computational burden of computer simulations, the maximum network size is limited to $N = 1,000$. This figure shows good agreement between analysis and simulation, in particular, when the number C of message replicas is small. However, we observe some deviation when the number C of message replicas is large.

Figures 20 and 21 seem to indicate that the large number C of message replicas is always desirable regardless of the network size N. However, this is untrue.

Figure 22 shows the average message delivery delay $D_{u,v}$ as a function of the number C of message replicas. In this figure, the load factor is set to $\alpha = 0.9$ to simulate highly loaded conditions. This figure clearly illustrates that the average message delivery delay $D_{u,v}$ is a concave function.

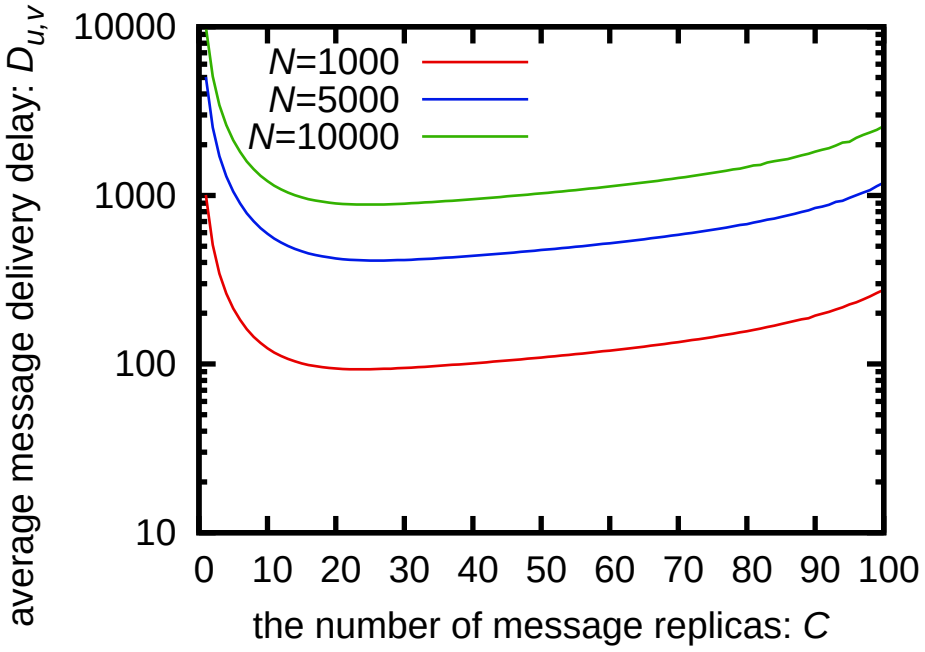

Figure 22: Relation between the number C of message replicas and average message delivery delay $D_{u,v}$.

The optimal number of message replicas is around $C = 20$ but it is almost independent of the network size N in this case.

Now we are ready to answer two research questions — how well or badly geographic DTN routing performs in a large-scale network and how the performance of geographic DTN routing is affected by the network topology.

Our observations regarding Fig. 20 answer the first question; somewhat surprisingly, geographic DTN routing is *scalable* in terms of the network size N since the average message delivery delay grows almost proportionally as the network size N increases, which is quite favorable property of geographic DTN routing.

Answering the second research question needs more explanation.

The second research question can be rephrased as follows: how the av-

erage message delivery delay $D_{u,v}$ in Fig. 20 is changed if *the average degree* is different (i.e., $k \neq 6$) and if *the degree distribution* of graph G is not binomial (e.g., power-law distribution as in scale-free networks). Except highly loaded conditions, the dominant factor of the replica delivery delay X_i is the transfer delay X_i^T rather than the queueing delay X_i^Q in Eq. (31). As Eq. (39) implies, the transfer delay is mostly determined by the average hitting time $H_{u,v}$, which is then determined solely by the ratio of *the number* $|E|$ *of edges* to *the degree* v *of the destination node* v. Namely, in geographic DTN routing under random walk mobility, the network topology has *limited* impact on the performance of geographic DTN routing; the average message delivery delay is mostly determined by the degree of the destination node.

3.5 Conclusion

In this chapter, we have presented a hybrid model of multiple-copy geographic DTN routing, which is composed of a continuous $M/M/1/PS$ queueing model and discrete multiple random walks on a large-scale network. We have approximately derived the average message delivery delay in a geographic DTN routing under random walk mobility on a large-scale network. We have analytically obtained the optimal number of message replicas (i.e., the number of copies per a message). Our findings includes that geographic DTN routing is scalable in terms of the network size N, and that the network topology has limited impact on the performance of geographic DTN routing except heavily loaded conditions.

Our future work includes extensive simulations under realistic scenarios to further validate our approximate analysis, and extension of our analysis to incorporate more realistic geographic DTN routing such as geometry-

aware routing algorithms, and other mobility patterns than the random walk.

4 Deriving the Mean Recurrence Time of Constrained Random WayPoint Mobility Model on a Graph

In this chapter, we derive the mean recurrence time of the CRWP mobility model to reveal the impact of mobility models on the performance of geographic DTN routing. The CRWP mobility model is an extension of the RWP (Random WayPoint) mobility model on a plane to the mobility model on a graph. In the CRWP mobility model, the following process is repeated; (1) an mobile agent randomly selects the destination node on the graph, and (2) the mobile agent moves following the shortest path from the current visited node to the destination node.

The various exploration, distribution and diffusion problems in information network can be reduced to single or multiple agents movement problems on a graph, and researches on characteristics of movement models on a graph have been actively conducted in recent years [18].

With regard to the random walk which is a typical mobility model, various characteristics (the sojourn probability, the hitting time, the mean recurrence time, etc.) have been analytically clarified.

Random walk on a graph is relatively easy to handle analytically because of its memoryless property, but characteristics of other mobility models on a graph that do not have memoryless property are not understood well enough.

In this chapter, we derive the mean recurrence time of the CRWP mobility model which is an extension of the RWP (Random WayPoint) mobility

model on a plane to the mobility model on a graph.

4.1 Analytic Model

We model the field comprising of multiple geographic locations and paths connecting those geographic locations as an undirected graph $G = (V, E)$ where vertices and edges correspond to geographic locations and paths, respectively.

We model the behavior of a mobile agent in geographic DTN routing as the CRWP mobility model on graph G. The source node of the mobile agent (the node that the mobile agent starts his movement at time $t = 0$) is denoted by $d_0 (\in V)$. In the CRWP mobility model, the following process is repeated; (1) an mobile agent randomly selects the destination node from the vertices V, and (2) the mobile agent moves toward its destination following the shortest path from the current visited node to its destination node.

4.2 Analysis

We derive the probability p_v that a mobile agent visits node $v (\in V)$ in the steady state and the expected time until the mobile agent departing node v revisits node v again (i.e., *the mean recurrence time*) R_v.

The mobile agent whose mobility pattern is the CRWP mobility model moves following the shortest path to the destination node randomly selected from the graph.

We denote a destination node selected at the $n (\geq 1)$ -th time by the CRWP mobility model as d_n, and the time that the mobile agent arrived at the destination node d_n as T_n respectively, where $T_0 = 0$.

Since the sojourn probability p_v of the node v is the rate at which the

mobile agent was visiting the node in the process of visiting the destination node sequentially, the sojourn probability p_v of the node v is given by

$$p_v = \frac{\sum_n \delta_v(d_{n-1}, d_n)}{\sum_n T_n - T_{n-1}} = \frac{\sum_n \delta_v(d_{n-1}, d_n)}{\sum_n l(d_{n-1}, d_n)}. \tag{42}$$

where $\delta_v(s,t)$ is a binary function that takes 1 if the node v is on the path from the node s to the node just before the node t in the shortest path from the node s to the node t, and 0 otherwise. $l(s,t)$ is the length of shortest path from the node s to the node t. In the CRWP mobility model, the destination node are randomly selected from all nodes in G with equal probability. Let b_v be the betweenness centrality of the node v in the graph $G = (V, E)$. Since the b_v is the proportion at which node v appears on the shortest path between all node of pairs, p_v is approximately given by

$$p_v \simeq \frac{b_v}{\sum_{s,t \in V} l(s,t)}, \tag{43}$$

Note that there are several definitions of betweenness centrality. In this chapter, the betweenness centrality b_v of node v is defined as

$$b_v = \sum_{s,t} \frac{\sigma_{s,t}(v)}{\sigma_{s,t}}, \tag{44}$$

where $\sigma_{s,t}$ is the number of shortest paths from node s to node t and $\sigma_{s,t}(v)$ is the number of paths passing through the node v among them.

Since p_v is the sojourn probability, it satisfies the normalization condition

$$\sum_v p_v = 1. \tag{45}$$

Therefore, the sojourn probability p_v at node v is obtained by using betweenness centrality b_v,

$$p_v \simeq \frac{b_v}{\sum_u b_u}. \tag{46}$$

If we represent the $i\,(\geq 1)$ -th recurrence time to the node v with the random variable X_i, then we have

$$\lim_{n\to\infty} \frac{n}{(X_1 + \cdots + X_n)} = p_v. \tag{47}$$

Therefore, the mean recurrence time R_v of node v is given by

$$R_v = E[X_i] = \frac{1}{p_v}. \tag{48}$$

4.3 Numerical Examples

The sojourn probability of each node (Eq.46) and the mean recurrence time (Eq.48) in the random network with 100 nodes and the average degree k generated by ER (Erdös-Rényi) model [17] are shown in Fig. 23 and Fig. 24, respectively.

In these figures, the node numbers are sorted so that the betweenness centrality b_v is in ascending order. Also, in these figures, the numerical results and simulation results are shown when the average degree k is 2, 4, and 6.

One can find from these figures that our analysis successfully captures the characteristics of the CRWP mobility model.

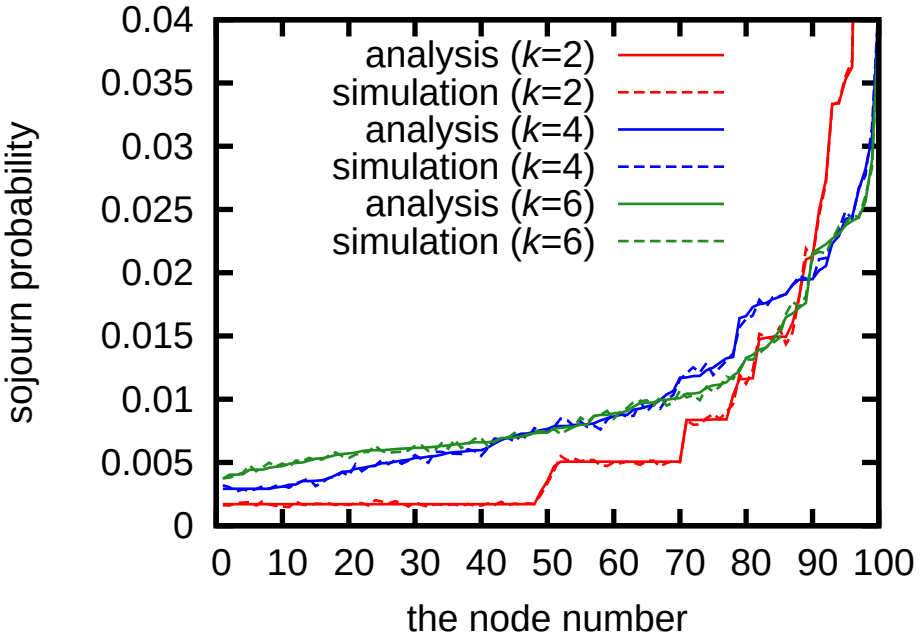

Figure 23: Relation between sojourn probability p_v and node v (the number of nodes $N = 100$)

4.4 Conclusion

In this chapter, we have derived the sojourn probability of each node in the steady state and the mean recurrence time of the CRWP mobility model. Our future challenges include deriving the average hitting time of the CRWP mobility model to reveal the impact of mobility models on the performance of geographic DTN routing and extension of our analysis to large-scale network.

5 Deriving Hitting Time of Constrained Random Way-Point Mobility Model on a Graph

In this chapter, we derive the hitting time of the CRWP mobility model (i.e., the expected value of the time for an agent on $G = (V, E)$ following

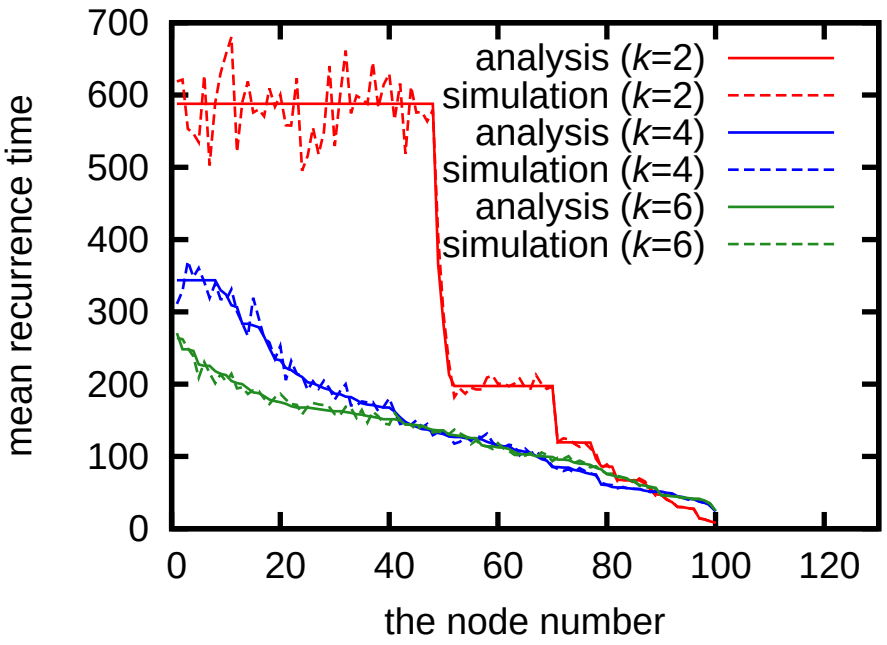

Figure 24: Relation between mean recurrence time R_v and node v (the number of nodes $N = 100$)

the CRWP mobility model from starting his movement on vertex $s \in V$ to reach vertex $t \in V$ at first).

5.1 Analysis

We consider the behavior of an agent moving discretely according to the CRWP mobility model on the undirected graph $G = (V, E)$.

The expected value of the time for the agent from starting a source node s to reach the end node t at first (hitting time) is denoted by $H_{s,t}$.

The agent moving according to the CRWP mobility model sequentially visits transit nodes $p_1, p_2, \ldots$ randomly selected from the graph, and arrives at the end node t in the process.

Since the selection of each transit node is independent, the sequence in which the agent visits transit nodes sequentially can be regarded as a kind

of random walk.

In other words, considering the weighted directed graph $G' = (V', E', w)$ with the shortest path between node pair $u, v \in V$ on the graph G as the vertex (Fig. 25), the movement on the graph G according to the CRWP mobility model can be represented by a discrete random walk on the graph G'.

However, unlike a simple discrete random walk, the transition time to an adjacent node on the graph G' is different depending on the link (the transition time is determined by the length of $(u, \ldots, v)$ which is the destination node). Therefore, the hitting time $H_{s,t}$ of the CRWP mobility model on the undirected graph G can be obtained from the hitting time of random walk on the weighted directed graph G'.

Specifically, the hitting time $H_{s,t}$ from the source node s to the end node t by the agent is given by the expected value of the time from a node $s' \in V' (= (s))$ to reach any node belonging to a node set $T' = \{v \in V' \,|\, t \in v\}$ at first in the weighted directed graph $G' = (V', E', w)$.

Here, let the shortest path from a node u to a node v be $P_{u,v}$, the k-th node of $P_{u,v}$ be $P_{u,v}(k)$, and the length of the shortest path $P_{u,v}$ be $l(u, v)$, $G' = (V', E', w)$ is defined as follows.

$$V' = \{P_{u,v} \,|\, u, v \in V\} \tag{49}$$

$$E' = \{(P_{u,v}, P_{v,p}) \,|\, u, v, p \in V\} \tag{50}$$

$$w((P_{u,v}, P_{v,p})) = \begin{cases} P_{v,p}^{-1}(t) - 1 & \text{if } t \in P_{v,p} \\ 0 & \text{if } u = v = p = s \\ l(u, v) & \text{otherwise} \end{cases} \tag{51}$$

where $P_{u,v}^{-1}(p)$ is the inverse function of $P_{u,v}(k)$.

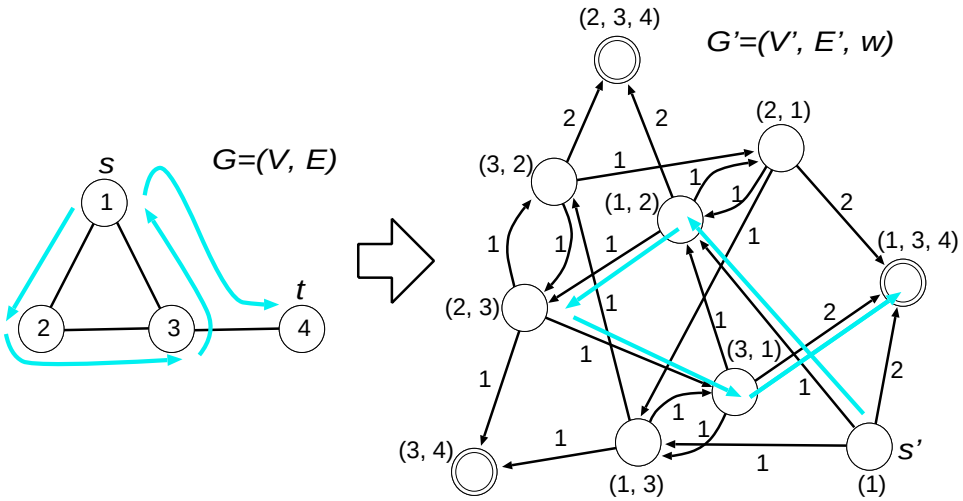

Figure 25: An example of the weighted undirected graph G' given by an undirected G with 4 nodes

Figure 25 shows an example of the weighted undirected graph G' given by an undirected graph G with 4 nodes.

The movement trajectory of a agent that the agent has started that source node $s = 1$ arrived at the end node $t = 4$ via the transit nodes $p_1 = 2, p_2 = 3, p_4 = 1, p_5 = 4$ selected by the CRWP mobility model is shown in this figure.

The expected value of the time from node s' to reach any node belonging to node set T' at first in the weighted directed graph $G' = (V', E', w)$, is given by the mean hitting time from the initial state to the absorption state in the continuous time Markov chain.

Specifically, we consider a continuous time Markov chain in which the state space is V' and the transition rate from state $i \in V'$ to state $j \in V'$ is

defined as follows.

$$\lambda_{i,j} = \begin{cases} \lambda_i \, p_{i,j} & \text{if } (i,j) \in E' \\ 0 & \text{otherwise} \end{cases} \tag{52}$$

$$\lambda_i = \sum_{j,\,(i,j)\in E'} p_{i,j} \, w((i,j)) \tag{53}$$

where $p_{i,j}$ is the transition probability from state i to state j.

The transition probability from state i $(= P_{u,v})$ to state j $(= P_{v,p})$ is given by

$$p_{i,j} = \frac{1}{(|V|-1)\, N_{v,p}}. \tag{54}$$

where $N_{u,v}$ is the number of shortest paths from a node u to a node v in graph G.

From this Markov chain, we can obtain mean hitting time from the initial state s' to the absorption state T'.

5.2 Numerical Examples

The hitting time from a source node s to an end node t in the random network with nodes $N = 30$ and the average degree $k = 2, 4, 6$ generated by ER (Erdös-Rényi) model [17] is shown in Fig. 26.

In this figure, the source node s is randomly chosen from the nodes whose betweenness centrality is the median of betweenness centrality for all nodes (i.e., node with typical betweenness centrality).

In this figure, the node numbers are sorted so that the hitting time $H_{s,t}$ is in ascending order.

Also, in this figure, the numerical results and simulation results are shown when the average degree k is 2, 4, and 6.

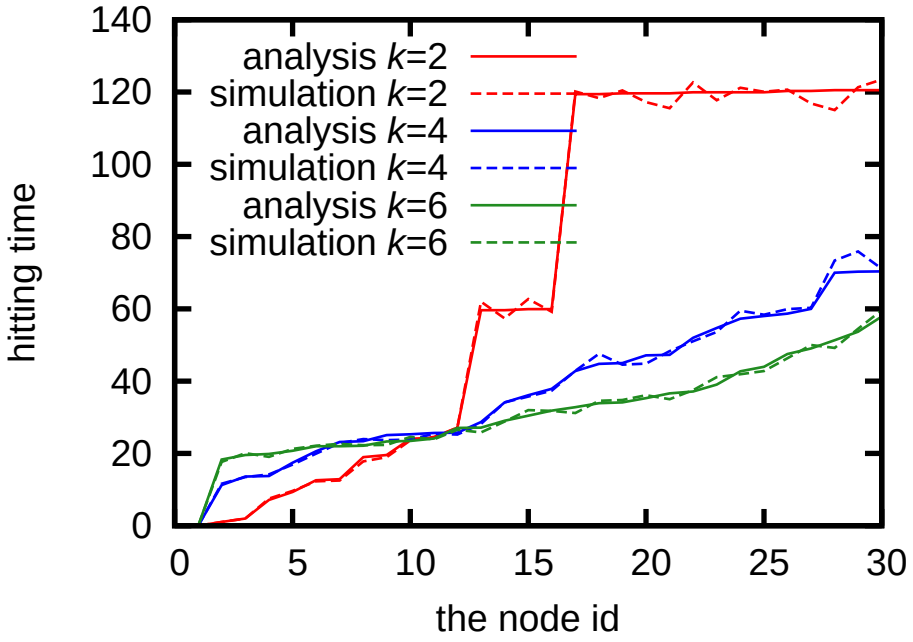

Figure 26: Relationship between the hitting time $H_{s,t}$ and node t (the number of nodes $N = 30$)

Comparison of numerical results and simulation results is plotted in Fig. 26, our analysis successfully captures the characteristics of the CRWP mobility model.

5.3 Conclusion

In this chapter, we have derived hitting time of the CRWP mobility model. Our future challenges include extension of our analysis to other mobility patterns and to large-scale network.

6 Conclusion

In this thesis, we have investigated geographic DTN routing with random mobile agents. We focus on random walks on a graph and the CRWP (Constrained Random WayPoint) mobility as random mobility.

First, we have derived the average and the distribution of message delivery delays in geographic DTN routing with the FIFO algorithm under one-time workload model and continuous workload model. We have analyzed the effect of system parameters — the number M of mobile agents on the field, the number K of message loadings at a geographic location, the message generation rate $\lambda_{u,v}$ and the number C of message replicas — on the average and the distribution of message delivery delays.

Second, we have approximately derived the average message delivery delay in a geographic DTN routing under random walk mobility on a large-scale network. Our findings includes that geographic DTN routing is scalable in terms of the network size N, and that the network topology has limited impact on the performance of geographic DTN routing except heavily loaded conditions.

Third, we have derived the sojourn probability of each node in the steady state and the mean recurrence time of the CRWP mobility model.

Fourth, we have derived the hitting time of the CRWP mobility model. Our finding includes that the CRWP mobility model can be regarded as a kind of random walk. The movement on the graph G according to the CRWP mobility model can be represented by a discrete random walk on the weighted directed graph $G' = (V', E', w)$.

Our future challenges include extension of our analysis to other mobility models for revealing the characteristics of the performance of geographic DTN routing and extension of our analysis to large-scale network.

Acknowledgments

I would like to express the deepest appreciation to Prof. Hiroyuki Ohsaki for his generous support, helpful feedback and insightful comments. Without his help and guidance, this thesis would not have been completed. I would like to express my appreciation to Prof. Naoki Kato Prof. Hiroyoshi Miwa, Prof. Tokio Taga and Prof. Motohiko Isaka. Their insightful comments and advises were invaluable. I would like to thank Mr. Yasuhiro Yamasaki, Mr. Ryo Hagihara, Ms. Natsuko Kawabata, Ms. Sumika Nishikawa and all members of the Large Scale Network Architecture Laboratory for their advice and warm support. Finally, I would like to thank my family for their support and encouragement.

References

[1] M. J. Khabbaz, C. M. Assi, and W. F. Fawaz, "Disruption-tolerant networking: A comprehensive survey on recent developments and persisting challenges," *IEEE Communications Surveys and Tutorials*, vol. 14, pp. 607–640, Jan. 2012.

[2] J. Burgess, B. Gallagher, D. Jensen, and B. N. Levine, "MaxProp: Routing for vehicle-based disruption-tolerant networks," in *Proceedings of the 25th IEEE International Conference on Computer Communicaitions (INFOCOM 2006)*, pp. 1–11, Apr. 2006.

[3] S. C. Nelson, M. Bakht, and R. Kravets, "Encounter-based routing in DTNs," in *Proceedings of the 28th IEEE International Conference on Computer Communications (INFOCOM 2009)*, pp. 846–854, Apr. 2009.

[4] M. Seki, K. Ogura, Y. Yamasaki, and H. Ohsaki, "Performance comparison of geographic DTN routing algorithms," in *Proceedings of the IEEE Signature Conference on Computers, Software, and Applications (Student Research Symposium) (COMPSAC 2015)*, pp. 617–620, July 2015.

[5] L. Lovász, "Random walks on graphs: a survey," *Combinatorics, Paul Erdos is eighty, Keszthely*, vol. 2, pp. 1–46, 1993.

[6] K. Efremenko and O. Reingold, "How well do random walks parallelize?," *Approximation, Randomization, and Combinatorial Optimization. Algorithms and Techniques*, vol. 5687, pp. 476–489, Aug. 2009.

[7] N. Uchida, K. Takahata, and Y. Shibata, "Disaster information system from communication traffic analysis and connectivity (quick report from japan earthquake and tsunami on march 11th, 2011)," in *Pro-*

ceedings of the 14th International Conference on Network-Based Information Systems (NBiS 2011), pp. 279–285, Sept. 2011.

[8] E. Gelenbe and F.-J. Wu, "Large scale simulation for human evacuation and rescue," *Computers & Mathematics with Applications*, vol. 64, pp. 3869–3880, Dec. 2012.

[9] S. Kitada, G. Hirakawa, G. Sato, N. Uchida, and Y. Shibata, "DTN based MANET for disaster information transport by smart devices," in *Proceedings of the 18th International Conference on Network-Based Information Systems (NBiS 2015)*, pp. 26–31, Sept. 2015.

[10] Y.-N. Lien, H.-C. Jang, and T.-C. Tsai, "A MANET based emergency communication and information system for catastrophic natural disasters," in *Proceedings of the 29th IEEE International Conference on Distributed Computing Systems Workshops (ICDCSW 2009)*, pp. 412–417, June 2009.

[11] D. Matsui, R. Hagihara, Y. Yamasaki, and H. Ohsaki, "Analysis of geographic DTN routing under random walk mobility model," in *Proceedings of the 41th IEEE Signature Conference on Computers, Software, and Applications (COMPSAC 2017)*, pp. 538–547, July 2017.

[12] R. Monteiro, W. Viriyasitavat, S. Sargento, and O. K. Tonguz, "A graph stracture approach to improving message dissemination in vehicular networks," *Wireless Networks*, vol. 23, pp. 2145–2163, Apr. 2016.

[13] S. Boccaletti, V. Latora, Y. Moreno, M. Chavez, and D.-U. Hwang, "Complex networks: Structure and dynamics," *Physics Reports*, vol. 424, no. 4, pp. 175–308.

[14] C. Stegehuis, R. van der Hofstad, and J. S. H. van Leeuwaarden, "Epidemic spreading on complex networks with community structures." https://www.nature.com/articles/srep29748.pdf, July 2016.

[15] M. Shahzamal, M. F. Pervez, M. A. U. Zaman, and M. D. Hossain, "Mobility models for delay tolerant network: A survey," *International Journal of Wireless & Mobile Networks (IJWMN)*, vol. 6, pp. 121–134, Aug. 2014.

[16] U. von Luxburg, A. Radl, and M. Hein, "Hitting and commute times in large graphs are often misleading." https://arxiv.org/abs/1003.1266.pdf, May 2011.

[17] P. Erdös and A. Rényi, "On random graphs i," *Publicationes Mathematicae (Debrecen)*, vol. 6, pp. 290–297, 1959.

[18] A. R. Ulrike von Luxburg and M. Hein, *Hitting and commute times in large graphs are often misleading*, pp. 1–33. Arxiv preprint arXiv:1003.1266, May 2011.

[19] 松井 大樹, 小倉 一峰, 山崎 康広, 大崎 博之, "拠点間 DTN ルーティングにおけるメッセージ配送遅延 の解析," **電子情報通信学会ソサイエティ大会 講演論文集** *(B-11-8)*, Sept. 2015.

[20] D. Matsui, Y. Yamasaki, and H. Ohsaki, "Analysis of message delivery delay in geographic DTN routing," in *Proceedings of the 40th IEEE Signature Conference on Computers, Software, and Applications (Doctoral Symposium) (COMPSAC 2016)*, pp. 496–497, June 2016.

[21] 松井 大樹, 萩原 涼, 大崎 博之, “拠点間 DTN ルーティングにおけるメッセージ配送遅延に関する一検討,” **電子情報通信学会ソサイエティ大会 講演論文集** *(B-16-4)*, p. 355, Sept. 2016.

[22] D. Matsui, R. Hagihara, Y. Yamasaki, and H. Ohsaki, “Deriving the average message delivery delay in geographic DTN routing,” *Technical Report of IEICE (IA2016-31)*, pp. 27–32, Nov. 2016.

[23] D. Matsui, R. Hagihara, Y. Yamasaki, and H. Ohsaki, “Deriving the average message delivery delay in geographic DTN routing under random walk mobility model,” **電子情報通信学会 総合大会 講演論文集** *(BS-1-29)*, pp. 56–57, Mar. 2017.

[24] 松井 大樹, 西川 純由, 山崎 康広, 大崎 博之, “大規模ネットワークにおける複製型拠点間 DTN ルーティングの特性解析に関する一検討,” **電子情報通信学会 ソサイエティ大会講演論文集** *(B-16-6)*, Sept. 2017.

[25] 松井 大樹, 大崎 博之, “グラフ上の制約付きランダムウェイポイント移動モデルの平均初回到着時間に関する一検討,” **電子情報通信学会 総合大会講演論文集** *(BS-XX-XX)*, pp. XX–XX, Mar. 2019.

List of Publications

1. 松井 大樹, 小倉 一峰, 山崎 康広, 大崎 博之, “拠点間 DTN ルーティングにおけるメッセージ配送遅延 の解析,” **電子情報通信学会ソサイエティ大会 講演論文集** *(B-11-8)*, Sept. 2015

2. D. Matsui, Y. Yamasaki, and H. Ohsaki, “Analysis of message delivery delay in geographic DTN routing,” in *Proceedings of the 40th IEEE Signature Conference on Computers, Software, and Applications (Doctoral Symposium) (COMPSAC 2016)*, pp. 496–497, June 2016

3. 松井 大樹, 萩原 涼, 大崎 博之, “拠点間 DTN ルーティングにおけるメッセージ配送遅延に関する一検討,” **電子情報通信学会ソサイエティ大会 講演論文集** *(B-16-4)*, p. 355, Sept. 2016

4. D. Matsui, R. Hagihara, Y. Yamasaki, and H. Ohsaki, “Deriving the average message delivery delay in geographic DTN routing,” *Technical Report of IEICE (IA2016-31)*, pp. 27–32, Nov. 2016

5. D. Matsui, R. Hagihara, Y. Yamasaki, and H. Ohsaki, “Deriving the average message delivery delay in geographic DTN routing under random walk mobility model,” **電子情報通信学会 総合大会 講演論文集** *(BS-1-29)*, pp. 56–57, Mar. 2017

6. D. Matsui, R. Hagihara, Y. Yamasaki, and H. Ohsaki, “Analysis of geographic DTN routing under random walk mobility model,” in *Proceedings of the 41th IEEE Signature Conference on Computers, Software, and Applications (COMPSAC 2017)*, pp. 538–547, July 2017

7. 松井 大樹, 西川 純由, 山崎 康広, 大崎 博之, “大規模ネットワークにおける複製型拠点間 DTN ルーティングの特性解析に関する一検討,” **電子情報通信学会 ソサイエティ大会講演論文集** *(B-16-6)*, Sept. 2017

8. 松井 大樹, 大崎 博之, “グラフ上の制約付きランダムウェイポイント移動モデルの平均初回到着時間に関する一検討,” **電子情報通信学会 総合大会 講演論文集** *(BS-XX-XX)*, pp. XX–XX, Mar. 2019